

1 Integrative multi-omics analysis of childhood aggressive behavior

2 RUNNING HEAD: Integrative multi-omics analysis of childhood aggressive behavior

3

4 Fiona A. Hagenbeek^{1,2,*}, Jenny van Dongen^{1,2,3}, René Pool^{1,2}, Peter J. Roetman⁴, Amy C. Harms^{5,6},

5 Jouke Jan Hottenga¹, Cornelis Kluit⁷, Olivier F. Colins^{4,8}, Catharina E.M. van Beijsterveldt¹, Vassilios

6 Fanos⁹, Erik A. Ehli¹⁰, Thomas Hankemeier^{5,6}, Robert R. J. M. Vermeiren^{4,11}, Meike Bartels^{1,2},

7 Sébastien Déjean¹², Dorret I. Boomsma^{1,2,3}

8

9 ¹Department of Biological Psychology, Vrije Universiteit Amsterdam, Amsterdam, the Netherlands.

10 ²Amsterdam Public Health research institute, Amsterdam, the Netherlands.

11 ³Amsterdam Reproduction & Development (AR&D) research institute, Amsterdam, the Netherlands.

12 ⁴LUMC-Curium, Department of Child and Adolescent Psychiatry, Leiden University Medical Center,

13 Leiden, the Netherlands

14 ⁵Division of Analytical Biosciences, Leiden Academic Center for Drug Research, Leiden University,

15 Leiden, the Netherlands

16 ⁶The Netherlands Metabolomics Centre, Leiden, The Netherlands.

17 ⁷Good Biomarker Sciences, Leiden, the Netherlands.

18 ⁸Department Special Needs Education, Ghent University, Ghent, Belgium.

19 ⁹Department of Surgical Sciences, University of Cagliari and Neonatal Intensive Care Unit, Cagliari,

20 Italy.

21 ¹⁰Avera Institute for Human Genetics, Sioux Falls, South Dakota, USA.

22 ¹¹Youz, Parnassia Psychiatric Institute, the Hague, the Netherlands.

23 ¹²Toulouse Mathematics Institute, University of Toulouse, CNRS, Toulouse, France.

24 * Correspondence: Fiona A. Hagenbeek, Department of Biological Psychology, Vrije Universiteit

25 Amsterdam, Van der Boechorststraat 7-10, 1081 BT Amsterdam, The Netherlands, Telephone: +31

26 (0)20 59 82974, E-mail: f.a.hagenbeek@vu.nl

27

28 N words main text: 9,014 words

29 N tables: 2 tables

30 N figures: 3 figures

31 Abstract

32 This study introduces and illustrates the potential of an integrated multi-omics approach in
33 investigating the underlying biology of complex traits such as childhood aggressive behavior. Using
34 multivariate statistical methods, we integrated 45 polygenic scores (PGSs) based on genome-wide
35 SNP data, 78,772 CpGs, and 90 metabolites for 645 twins (cases=42.0%, controls=58.0%). The single-
36 omics models selected 31 PGSs, 1614 CpGs, and 90 metabolites, and the multi-omics biomarker
37 panel comprised 44 PGSs, 746 CpGs, and 90 metabolites. The predictive accuracy in the test ($N=277$,
38 cases=42.2%, controls=57.8%) and validation data ($N=142$ participants from a clinical cohort,
39 cases=45.1%, controls=54.9%) ranged from 43.0% to 57.0% for the single- and multi-omics models.
40 The average correlations across omics layers of omics traits selected for aggression in single-omics
41 models ranged from 0.18 to 0.28. In the multi-omics model higher correlations were found and we
42 describe five sets of correlational patterns with high absolute correlations ($|r| \geq 0.60$) of aggression-
43 related omics traits selected into the multi-omics model, providing novel biological insights.

44 **Keywords:** Childhood aggression; multi-omics; polygenic scores; genetic nurturing; DNA
45 methylation; metabolomics.

46 Introduction

47 Omics studies can lead to an improved understanding of the biological mechanisms contributing
48 to mental health and disorders (Jakovljevic and Jakovljevic 2019). Different omics technologies, e.g.,
49 genomics, epigenomics, transcriptomics, or metabolomics, assess different aspects of the
50 development and progression of complex traits and disorders. The analysis of a single omics layer
51 provides a unique, but incomplete, picture of the underlying biology, whereas studies combining
52 multiple omics layers may lead to more comprehensive insights into human biology, because the
53 different omics layers are interrelated and interact (Wörheide et al. 2021). Multi-omics analyses can
54 aid in biomarker discovery, diagnosis, patient classification or subtyping, evaluation of treatment
55 response and uncovering novel insights into disease biology (Pinu et al. 2019; Subramanian et al.
56 2020).

57 Here, we present an integrative multi-omics analysis of childhood aggressive behavior. Human
58 aggression is a complex and heterogenous behavior encompassing hostile, destructive, or injurious
59 behavior aimed at causing physical or emotional harm to others (Anderson and Bushman 2002;
60 Siever 2008). In several disruptive behavioral disorders, such as conduct and oppositional defiant
61 disorders or intermittent explosive disorder, inappropriate levels of aggressive behavior are
62 observed (Radwan and Coccaro 2020). In humans, high co-occurrence with other social, behavioral,
63 and emotional problems is reported (Bartels et al. 2018; Whipp et al. 2021a). Childhood aggressive
64 behavior puts a burden on children and their parents/caretakers, and is predictive of multiple
65 adverse outcomes later in life, such as antisocial personality disorder (Whipp et al. 2019), criminal
66 convictions (Kassing et al. 2019), lower educational attainment (Vuoksimaa et al. 2020), or negative
67 interpersonal relationships (Fergusson et al. 2005).

68 Large-scale genome-wide association (GWA) studies on aggression have not yet identified
69 significant single nucleotide polymorphisms (SNPs) (Odintsova et al. 2019; Ip et al. 2021). Gene-
70 based analysis for childhood aggression yielded three significantly associated genes (*ST3GAL3*,

71 *PCDH7*, and *IPO13*) (Ip et al. 2021). The polygenic score for childhood aggression does not only
72 significantly explain childhood aggressive behavior at age 7 (Ip et al. 2021), but it also associated
73 with aggression at age 12 to 41 in a Dutch sample and age 38 to 48 in an Australian sample (van der
74 Laan et al. 2021). Small-scale epigenetic studies (sample size range: 41-260) showed that DNA
75 methylation differences in various tissues associated with aggression and related traits in children
76 and adults (Guillemin et al. 2014; Cecil et al. 2018b, a; Mitjans et al. 2019). The first large-scale
77 epigenome-wide association analyses (EWAS) meta-analysis across child and adult cohorts (N =
78 15,324) reported 13 significant sites in peripheral blood for broad aggression across the lifespan (van
79 Dongen et al. 2021). Metabolomics studies (sample size range: 77-725) detected plasma and serum
80 metabolites associated with aggression and related traits in adults (Gulsun et al. 2016; Chen et al.
81 2020; Whipp et al. 2021b). And a study in 1,347 twins and 183 clinical cases found significant
82 associations of urinary metabolites with childhood aggression (Hagenbeek et al. 2020). These single
83 omics approaches hint at potentially important biological pathways for human aggression, with most
84 of these findings awaiting replication.

85 In this study, we aim to integrate multiple omics layers to construct a multi-omics biomarker
86 panel for childhood aggressive behavior and explore the correlations among the omics traits
87 included in this panel. We collected biological samples in a subproject of ACTION (Aggression in
88 Children: Unraveling gene-environment interplay to inform Treatment and InterventiON strategies):
89 the ACTION Biomarker Study (Boomsma 2015; Bartels et al. 2018; Hagenbeek et al. 2020). The
90 ACTION Biomarker Study comprised a cohort of twins from the Netherlands Twin Register (NTR)
91 (Ligthart et al. 2019) and a clinical cohort of children referred to a youth psychiatry clinic (LUMC-
92 Curium, the Netherlands). The genome-wide SNP and DNA methylation (Illumina EPIC 850K array)
93 data, and the urinary amines and organic acids as measured in these cohorts were previously
94 included in a genome-wide genetic and epigenetic association study and a metabolomics study of
95 (childhood) aggression (Hagenbeek et al. 2020; van Dongen et al. 2021; Ip et al. 2021). We expand
96 on these single-omics studies, by integrating this data with a third metabolomics dataset, focusing

97 on urinary steroid hormones, and calculating transmitted and non-transmitted polygenic scores
98 (PGSs) for childhood aggression and a series of genetically correlated traits, such as Attention-Deficit
99 Hyperactivity Disorder (ADHD), smoking, and intelligence. The non-transmitted PGSs assess the
100 indirect effects of genetic variants that were not transmitted from parents to offspring, i.e., genetic
101 nurture, and capture the effects of the environment created by parents beyond the genetic
102 intergeneration transmission (Kong et al. 2018). Thus, if alleles not transmitted from parents to
103 offspring affect offspring outcomes, this indicates that the offspring's home-environment is
104 influenced by parental genotypes, and the home-environment in turn affects offspring outcomes
105 (Branje et al. 2020).

106 We employed an analytical design comprising three phases: 1) single-omics analyses; 2) pairwise
107 cross-omics analyses; and 3) multi-omics analyses (Fig. 1) (Duruflé et al. 2020). First, we built single-
108 omics biomarker panels in the twin cohort, with 70% of the twin data for model training, 30% of the
109 twin data for model testing, and the clinical cohort for model validation. Second, we examined the
110 overall pairwise cross-omics correlations and the pairwise correlations of those omics traits selected
111 by the single-omics models in the training data. Third, using the same data split for model training,
112 testing and validation, we compared three multi-omics models, with different assumptions on the
113 correlations among the omics traits and describe the multi-omics correlations of the selected omics
114 traits.

115 Materials and methods

116 Study population and procedures

117 Participants included 1,494 twins (747 complete pairs) from the Netherlands Twin Register
118 (Ligthart et al. 2019), and 189 children referred to the LUMC-Curium youth psychiatry clinic in the
119 Netherlands that took part in the ACTION Biomarker Study (Aggression in Children: Unraveling gene-
120 environment interplay to inform Treatment and InterventiON strategies) (Boomsma 2015; Bartels et
121 al. 2018; Hagenbeek et al. 2020). Both cohorts collected first-morning urine samples and buccal-cell

122 swabs with standardized protocols (for details, see **Appendix A**). In the twin cohort, we also
123 collected buccal-cell swabs from parents and siblings of the twins. The current study included
124 participants if they had aggression status, complete omics data for all three omics layers, and all
125 relevant covariates (**Table S1**). Parents provided written informed consent for their children and twin
126 parents provided written informed consent for their own participation. Study approval was obtained
127 from the Central Ethics Committee on Research Involving Human Subjects of the VU University
128 Medical Center, Amsterdam (NTR 25th of May 2007 and ACTION 2013/41 and 2014.252), an
129 Institutional Review Board certified by the U.S. Office of Human Research Protections (IRB number
130 IRB00002991 under Federal-wide Assurance- FWA00017598; IRB/institute codes), and the Medical
131 Ethical Committee of Leiden University Medical Center (B17.031, B17.032 and B17.040).

132 **Aggressive behavior**

133 Mothers and teachers rated aggressive behavior on the Aggressive Behavior syndrome scale of
134 the Achenbach System of Empirically Based Assessment (ASEBA) Child Behavior Checklist (CBCL) or
135 Teacher Report Form (TRF) (Achenbach et al. 2017). We have described selection and definition of
136 aggression cases and controls previously (Hagenbeek et al. 2020). In brief, we selected twin pairs
137 based on concordance (case-case or control-control) and discordance (case-control pairs) for
138 mother- (93%) or teacher-rated (7%) aggressive behavior at ages 3, 7, and/or 10 years. We matched
139 concordant control pairs on postal code to the case-case and case-control pairs, and collection of
140 biological samples within regions in the Netherlands was around the same time. Cases were defined
141 by mother- or teacher-rated sex- and age-specific T-scores of 65 or higher (subclinical levels), or on
142 mother-rated age-specific thresholds on the item scores at age 3 (≥ 13), age 7 (≥ 5), or age 10 (≥ 4)
143 ($N = 388$, **Table S1**). We denoted individuals with scores below these thresholds as controls ($N = 534$,
144 **Table S1**). In the clinical cohort, children with a parent-rated sex-specific T-score of ≥ 70 (clinical
145 levels) were classified as cases ($N = 64$), and children with T-scores of < 65 were classified as low
146 scoring controls ($N = 78$, **Table S1**). We excluded children with T-scores in the subclinical range (T-
147 scores of ≥ 65 and < 70) from this study ($N = 35$).

148 Omics measurements

149 Details on omics measurements are included in **Appendix B**. Genotyping was performed on
150 Affymetrix Axiom or Illumina GSA arrays (Ehli et al. 2017; Beck et al. 2019), and genome-wide SNP
151 data were available for 3,334 participants, including 1,702 parents and siblings of twins (AXIOM =
152 909, GSA = 2,425). Transmitted and non-transmitted polygenetic scores (PGS) were calculated for
153 childhood aggression and 14 other traits that showed a significant ($p < 0.02$) genetic correlation of \leq
154 -0.40 or ≥ 0.40 with childhood aggression (Ip et al. 2021) (**Table 1**). Thus, in total we calculated 45
155 PGSs: a transmitted (15), non-transmitted by mother (15), and non-transmitted by father (15) PGS
156 for each trait. The effects of sex, age at biological sample collection, genotyping platform, and the
157 first 10 genetic principal components (PCs) were regressed on the standardized PGSs and we
158 included residuals in the analyses.

159 Genome-wide DNA methylation was measured on the Infinium MethylationEPIC BeadChip Kit
160 (Illumina, San Diego, CA, USA (Moran et al. 2016)). Quality Control (QC) and normalization were
161 carried out with pipelines developed by the Biobank-based Integrative Omics Study (BIOS)
162 consortium (Sinke et al.). From the 787,711 autosomal methylation probes that survived QC, the top
163 10% most variable probes were included in the analyses (**Data S1**). Residual methylation levels were
164 obtained by regressing the effects of sex, age, percentages of epithelial and natural killer cells, EPIC
165 array row, and bisulfite sample plate, from the methylation β -values.

166 Urinary metabolomics data were generated on: 1) a liquid chromatography mass spectrometry
167 (LC-MS) platform targeting amines; 2) a LC-MS platform targeting steroid hormones; and 3) a gas
168 chromatography (GC) MS platform targeting organic acids. We excluded metabolites with a relative
169 standard deviation of the QC samples larger than 15% and retain 60 amines, 10 steroids, and 20
170 organic acids in our analyses. After QC, we normalized metabolite levels to the sample-median and
171 inverse normal rank transformed. We analyzed residuals obtained by regressing the effects of sex
172 and age on the normalized and transformed urinary metabolites.

173 Statistical analyses

174 To define multi-omics biomarker panels capable of discriminating between cases and controls
175 and explore the correlations among the omics traits included in these panels, we employed an
176 analytical design comprising three phases: 1) single-omics analyses; 2) pairwise cross-omics analyses;
177 and 3) multi-omics analyses (**Fig. 1**). To avoid overfitting of the single- and multi-omics models, we
178 randomly split the twin sample at the twin pair level into two subsets: 70% of the data for model
179 training (training data), and 30% of the data for model testing (test data; **Table 2**). The clinical
180 validity of the final single- and multi-omics models was evaluated in the clinical cohort (validation
181 data; **Table 2**). We carried analyses out in the mixOmics R package (version 6.12.1) implemented in
182 the R programming language (version 4.0.2) (R Core Team; Rohart et al. 2017).

183 Phase 1: Single-omics analyses

184 *Univariate polygenic score analyses*

185 In the training data, we first associated the transmitted- and non-transmitted PGSs with
186 childhood aggression through generalized estimating equation (GEE) models. GEE models tested the
187 association of each transmitted and non-transmitted PGS separately on the continuous mother-
188 rated sum scores of the ASEBA CBCL Aggressive Behavior syndrome scale as assessed at the time of
189 biological sample collection. All models included sex, age, genotype array, and the first 10 genetic
190 principal components as covariates. We corrected for the correlation structure within families by
191 using the “exchangeable” correlation structure, obtaining robust variance estimators (Rogers and
192 Stoner 2016). A False Discovery Rate (FDR) of 5% for 45 PGSs was used to correct for multiple testing
193 (p.adjust function in R), setting the significance threshold to $q \leq 0.05$, i.e., 5% of the significant
194 results will be false positives (Benjamini and Hochberg 1995).

195 *Multivariate single-omics models*

196 To get a first insight into the dimensionality of the metabolomics data (90 variables), DNA
197 methylation data (78,772 variables), and the PGSs (45 variables), we ran Principal Component

198 Analysis (PCA) within each omics layer in the training data (**Table S2**). To assess the ability of each of
199 the three omics layers to correctly classify aggression status, we applied Partial Least Square
200 Discriminant Analysis (PLS-DA) in the training data. PLS-DA involves iteratively constructing
201 successive latent components, where each component is a linear combination of the included omics
202 traits (Rohart et al. 2017). For each component, PLS-DA aims to maximize the covariance between
203 the residual X matrix, containing the omics data, and the Y matrix, containing the sample
204 classification (i.e., case-control status coded as a dummy variable). The mixOmics software requires
205 a user-defined maximum number of components in PLS-DA models. We chose this maximum based
206 on the number of PCs as determined by the elbow method in the PCA (**Fig. S1; Table S2**). To find the
207 optimal number of components to keep in each PLS-DA model, we employed 10-fold cross-validation
208 (CV) with 100 repeats (*perf* function; **Table S3; Fig. S2**).

209 Next, we applied sparse PLS-DA (sPLS-DA) to reduce the number of traits in each omics layer
210 contributing to each component. sPLS-DA includes Least Absolute Shrinkage and Selection Operator
211 (LASSO) penalization (e.g., $L1$ penalization). LASSO shrinks the coefficients of less importance, often
212 highly correlated, traits to zero, removing these traits from the model (Tibshirani 1996). Thus, for
213 each component, sPLS-DA finds the maximum covariance between the residual X matrix containing a
214 subset of the omics data with non-zero coefficients (variable selection) and the Y matrix (Lê Cao et
215 al. 2011). We assessed the trait selection via 10-fold CV with 100 repeats (*tune* function), keeping at
216 least two components in the final model (**Table S3; Fig. S3**). CV again obtained the performance of
217 the final sPLS-DA model using the *perf* function (10 folds, 100 repeats; **Table S3; Fig. S4**).

218 The ability of the final single-omics models to accurately predict out-of-sample case-control
219 status was evaluated in the test and validation data (*predict* function). For each new observation in
220 the test and validation data, this function calculates the predicted class (case/control) by estimating
221 their predicted dummy variable (of the case-control status) using the maximum, Mahalanobis, or
222 Centroids (Euclidian) distance (see Rohart et al. 2017). When using the maximum distance, the

223 predicted class of a new observation is the class for which we observed the largest predicted dummy
224 value. Both the Mahalanobis and centroids distances are centroid-based distances that predict the
225 class of a new observation, so that the distance between its centroid and predicted scores is
226 minimal. To out-of-sample case-control status, we used the best performing prediction distance, as
227 was determined during model training (see **Table S3**).

228 The misclassification rates of the models, that combine the number of cases classified as controls
229 (false negative rate) and the number of controls classified as cases (false positive rate), was used to
230 evaluate how well the final models predicted case-control status. We employed a balanced
231 misclassification rate, the balanced error rate (BER), that corrects for imbalances in the number of
232 cases and controls. We used a confusion matrix, comparing the true cases and controls with the
233 predicted cases and controls, to calculate the sensitivity (number of cases correctly classified as
234 cases [true positive rate]), specificity (number of controls correctly classified as controls [true
235 negative rate]), and accuracy (overall correct classification). As an alternative, Receiver Operating
236 Characteristic (ROC) analysis assessed the Area Under the Curve (AUC) in both the test and
237 validation data. We obtained the ROC curve per component.

238 **Phase 2: Pairwise cross-omics analyses**

239 To highlight pairwise cross-omics relationships (i.e., DNA methylation-metabolomics, PGSS-
240 metabolomics, and PGSS-DNA methylation), Partial Least Squares (PLS) regression models were
241 constructed in canonical mode in the training data. Similar to canonical correlation analysis,
242 canonical PLS regression aims to find linear combinations of the variables (canonical variates) to
243 reduce the dimensionality of the data while maximizing the covariance between the variates (Rohart
244 et al. 2017). CV has not yet been implemented for PLS in canonical mode. Consequently, we kept the
245 smallest number of components as kept in either of the respective single-omics models (**Table S3**).
246 Therefore, we included 3 components for the DNA methylation-metabolomics model, and 2
247 components for the PGS-metabolomics and PGS-DNA methylation models.

248 The PLS models were run with two different numbers of included omics traits, 1) a PLS model that
249 included all 45 PGs, 78,772 CpGs, and 90 metabolites (model 1), and 2) a PLS model that only
250 included the 36 PGs, 1,614 CpGs, and 90 metabolites that were selected by the single-omics sPLS-
251 DA models (model 2; **Data S2**). Model 1 provides insight into the correlations among all omics traits,
252 while model 2 provides insight into the correlations of those omics traits that best contribute to
253 aggression case-control classification in the single-omics sPLS-DA models. On the omics traits
254 included in model 2, we performed hierarchical clustering with the Ward linkage algorithm on
255 Euclidean distances of the PLS variates and used the ‘dendextend’ R-package (Galili 2015) to extract
256 the two largest clusters for both of the omics layers included in the PLS models.

257 Phase 3: Multi-omics analyses

258 The multi-omics analysis was conducted through Data Integration Analysis for Biomarker
259 discovery using Latent cOmponents (DIABLO) in the training data. DIABLO extends PLS-DA to multi-
260 block PLS-DA (MB-PLS-DA), that aims at identifying correlated traits from multiple omics layers that
261 maximize the sample classification (Singh et al. 2019). The method requires a user-defined ‘design
262 matrix’, that specifies the expected correlations among the omics layers. The symmetric design
263 matrix has the number of rows and columns equal to the number of omics layers (i.e., 3), and
264 contains values between 0 and 1. A ‘full’ design matrix denotes strong positive correlations among
265 the omics layers and sets the values among omics layers close to or equal to one. A ‘null’ design
266 matrix denotes weak or no correlations among omics layers by setting values close to or equal to
267 zero. The full design matrix optimizes correlations among the omics layers, while the null design
268 matrix optimizes the discrimination between samples (Rohart et al. 2017; Singh et al. 2019; Duruflé
269 et al. 2020). We can also specify a design matrix with the empirical correlations among the omics
270 layers.

271 We compared a multi-omics model with an empirical design matrix (based on the correlations
272 obtained from the model 1 pairwise cross-omics PLS models; **Table S4**) to models with a null or full

273 design matrix. Based on the results of the single-omics sPLS-DA models (**Table S5**), we chose the
274 maximum number of components to include in the MB-PLS-DA models. We determined the optimal
275 number of components to keep in the MB-PLS-DA model with 10-fold CV and 100 repeats (*perf*
276 function; **Fig. S5**). We assessed the trait selection per component per omics layer via 5-fold CV with
277 50 repeats (*tune* function; **Table S5**; **Fig. S6**). Performance of the final MB-sPLS-DA model was
278 assessed with 5-fold CV (50 repeats; **Table S5**; **Fig. S7**).

279 The ability of the final multi-omics models to predict out-of-sample case-control status was
280 evaluated in the test and validation data (*predict* function), using the best performing prediction
281 distance as was determined during model training (see **Table S5**). The final multi-omics models were
282 evaluated by their balanced error rates, and the sensitivity, specificity, and accuracy of the models
283 were calculated from their confusion matrices. In the multi-omics models, we calculated the ROC
284 curves per component for each omics layer.

285 Biological characterization

286 To facilitate biological interpretation, we describe the correlations of the PGSSs, CpGs, and
287 metabolites, that were selected by the single-omics sPLS-DA models and those selected by the multi-
288 omics MB-sPLS-DA models. For the multi-omics MB-sPLS-DA models we also identified correlation
289 patterns that included high absolute correlations ($|r| \geq 0.60$) between omics traits of at least two
290 omics layers. To test for enrichment of methylation sites previously associated with other traits, we
291 performed trait enrichment analysis for all traits (619) in the EWAS atlas on the 18th of June 2021 (Li
292 et al. 2019). CpGs served as input for the trait enrichment analysis if 20 or more unique CpGs were
293 selected into the single-omics sPLS-DA model, the multi-omics MB-sPLS-DA models, or included in a
294 multi-omics MB-sPLS-DA high correlation pattern. When fewer than 20 CpGs were selected, we
295 manually retrieved the trait associations with the CpGs from the EWAS atlas. Similarly, we
296 performed trait enrichment analysis or manual retrieval of the CpGs included in the clusters as

297 identified for the pairwise cross-omics analyses for all traits (618) in the EWAS atlas on the 1st of July
298 2021.

299 Results

300 Polygenic prediction

301 Transmitted and non-transmitted PGSs for childhood aggression and 13 other traits were
302 individually not significantly associated with aggressive behavior after multiple testing correction
303 (**Data S3**). The transmitted PGS for ADHD were significantly associated with aggressive behavior ($\beta =$
304 1.16 , $SE = 0.26$, $q = 0.0003$), while the non-transmitted PGSs were not (mother: $\beta = -0.22$, $SE = 0.24$, q
305 $= 0.83$; father: $\beta = 0.02$, $SE = 0.23$, $q = 0.98$), showing that genetic liability for ADHD associates with
306 increased levels of aggressive behavior.

307 Single-omics models for childhood aggression

308 We built single-omics biomarker panels for childhood aggressive behavior based on sPLS-DA
309 models including PGSs, DNA methylation, or metabolomics data. After extensive cross-validation the
310 optimal models included 11 transmitted and 25 non-transmitted PGSs (2-component model), across
311 all components, 1,614 CpGs (6-component model), and all 90 metabolites (2-component model)
312 (**Table S3; Data S2**). All three single-omics models showed poor separation of aggression cases and
313 controls on all components (**Fig. S8**). Prediction in the test data showed that model performance was
314 at most slightly better than random assignment of case-control status for the PGSs (BER = 0.51-0.51,
315 range is for the different components), for the DNA methylation data (BER = 0.44-0.51), and for the
316 metabolomics data (BER = 0.52-0.54; **Table S6**). In the validation data, the average classification
317 accuracy was better for the metabolomics model (BER = 0.48-0.51), but not for the PGS (BER = 0.50-
318 0.51) and DNA methylation models (BER = 0.48-0.58; **Table S6**). Similarly, the single-omics models
319 had low sensitivity and specificity in both the test and validation data and ROC curve analyses
320 showed the AUCs ranged from 0.48 to 0.58 in the test data and from 0.39 to 0.58 in the validation

321 data (**Table S6**). As a result, we observed a low degree of separation among cases and controls in
322 both the test and validation data (**Fig. S9- S10**).

323 Out of the 36 selected PGSs, 11 transmitted and 16 non-transmitted PGSs (75%) were selected
324 with high stability, i.e., included in 80% of the cross-validation rounds (**Data S2**). PGSs that were
325 consistently included in the sPLS-DA model for childhood aggression, included the transmitted and
326 both non-transmitted PGSs for childhood aggression and number of cigarettes per day, the
327 transmitted and non-transmitted by mother PGSs for ADHD, age at first birth, Major Depressive
328 Disorder (MDD), insomnia, loneliness, and Educational Attainment (EA), the transmitted and non-
329 transmitted by father PGSs for smoking initiation, both non-transmitted PGSs for self-reported
330 health, the transmitted PGSs for wellbeing spectrum and age of smoking initiation, the non-
331 transmitted by mother PGSs for Autism Spectrum Disorder (ASD) and intelligence, and the non-
332 transmitted by father PGS for childhood IQ. The remaining PGSs included in the final sPLS-DA model
333 had a stability ranging from 50%-78%, and included the non-transmitted by mother (childhood IQ,
334 wellbeing spectrum, age at smoking initiation, and smoking initiation) and non-transmitted by father
335 scores (intelligence, MDD, ADHD, wellbeing spectrum, and ASD).

336 In contrast, only 56 out of the 1,614 CpGs (3.5%) were selected with high stability (range = 0.1%-
337 97.9%; **Data S2**). We performed trait enrichment analyses against all reported associations in the
338 EWAS atlas for all selected CpGs in the sPLS-DA model. We observed the strongest enrichment for
339 glucocorticoid exposure (i.e., administration of corticosteroid medication (Braun et al. 2019); OR =
340 18.02, $p = 5.34 \times 10^{-158}$), and household socioeconomic status in childhood (OR = 9.88, $p = 1.18 \times 10^{-13}$;
341 **Table S7**). In addition, we saw enrichment for many other traits, not obviously related to aggressive
342 behavior. All 90 metabolites selected by the sPLS-DA model were selected with high stability (**Data**
343 **S2**).

344 Pairwise cross-omics models

345 The average correlations between each omics layer from pairwise PLS cross-omics models
346 including all omics traits, i.e., the correlation among all PLS variates of all components
347 simultaneously, were $r = 0.18$ ($q = 3.19 \times 10^{-15}$) for DNA methylation-metabolomics, $r = 0.28$ ($q =$
348 7.97×10^{-24}) for PGSS-metabolomics, and $r = 0.29$ ($q = 2.30 \times 10^{-26}$) for PGSS-DNA methylation (**Table**
349 **S4**). We observed a decrease in the average correlations between the PGSSs and CpGs ($r = 0.28$, $q =$
350 9.57×10^{-24}), but not between the PGSSs and metabolites or the CpGs and metabolites, when including
351 only the omics traits selected through single-omics sPLS-DA in the pairwise PLS cross-omics models
352 (**Table S4**). Overall, these correlations suggest that omics traits for childhood aggression from
353 different omics layers capture largely independent information and that childhood aggression is
354 associated with variation across different omics layers.

355 Pairwise DNA methylation-metabolomics correlations

356 In the pairwise DNA methylation-metabolomics model, we used hierarchical clustering and found
357 two clusters of CpGs and of metabolites (**Fig. 2a**; **Data S4**). The DNA methylation cluster 1 contains
358 1,151 (71.3%) of the CpGs selected by the sPLS-DA models for childhood aggression. These CpGs
359 located across the genome, have the largest number of CpGs on chromosome 1 ($N = 112$, 9.7%), and
360 chromosome 2 ($N = 93$, 8.1%), and the strongest trait enrichments for these CpGs were observed for
361 household socioeconomic status in childhood ($OR = 12.48$, $p = 4.20 \times 10^{-14}$), and psoriasis ($OR = 3.70$, p
362 $= 1.18 \times 10^{-10}$; **Table S8**). The 463 (28.7%) CpGs included in cluster 2 are also located across the
363 genome, with chromosome 3 ($N = 43$, 9.3%), and chromosome 4 ($N = 39$, 8.4%) containing the
364 largest amount of cluster 2 CpGs, that show the strongest trait enrichment for glucocorticoid
365 exposure ($OR = 51.25$, $p \leq 1.00 \times 10^{-308}$; **Table S8**). Metabolite cluster 1 contains 69 (76.7%) of the
366 metabolites, including 55 amines, 7 organic acids and 7 steroids, while metabolite cluster 2 contains
367 21 metabolites (23.3%), including 5 amines, 13 organic acids, and 3 steroids.

368 The correlation of the CpGs included in cluster 1 with metabolites ranges from -0.20 to 0.19 (r M
369 = -0.001, r SD = 0.02; **Fig. 2a; Data S4-S5**). The correlations of the cluster 1 CpGs with the cluster 1
370 metabolites are lower (r M = -0.005, r SD = 0.02, r range = -0.19-0.19) than those observed with the
371 cluster 2 metabolites (r M = 0.01, r SD = 0.01 r range = -0.20-0.19). The CpGs included in cluster 2
372 have correlations ranging from -0.23 to 0.18 with metabolites (r M = -0.05, r SD = 0.01), with
373 predominantly negative correlations observed between these CpGs and the amines included in
374 metabolite cluster 1 (r M = -0.095, r SD = 0.01, r range = -0.23-0.18; **Fig. 2a; Data S4-S5**). We
375 observed the highest absolute correlations ($|r| \geq 0.20$) between metabolites of cluster 1 and CpGs
376 included in cluster 2, specifically, the amines 3-methoxytyramine (r M = -0.21, r SD = 0.01, r range: -
377 0.23 to 0.20), asymmetric dimethylarginine (ADMA, r M = -0.20, r SD = 0.002, r range: -0.21 to -0.20),
378 L-glutamic acid (r = -0.20), L-phenylalanine (r M = -0.20, r SD = 0.003, r range: -0.21 to -0.20), O-
379 acetyl-L-serine (r = -0.20), and symmetric dimethylarginine (SDMA, r M = -0.21, r SD = 0.004, r range:
380 -0.22 to -0.20) show negative correlations with these CpGs (**Fig. 2a; Data S4-S5**), showing that
381 increased levels of these urinary metabolites associated with hypomethylation at cluster 2 CpG sites.

382 **Pairwise PGSs-metabolomics correlations**

383 Hierarchical cluster of the pairwise PGSs-metabolomics model identified two clusters of PGSs and
384 two clusters of metabolites (**Fig. 2b; Table S9**). The PGS cluster 1 contains 23 of the PGSs (63.9%)
385 selected by the sPLS-DA model for childhood aggression (**Fig. 2b; Table S9**). This cluster contains 8
386 transmitted PGSs, 9 PGSs non-transmitted by mother and 6 non-transmitted by father, including the
387 transmitted and both non-transmitted PGSs for ADHD, childhood aggression, number of cigarettes
388 per day, and MDD, the transmitted and non-transmitted by mother PGSs for insomnia, both non-
389 transmitted PGSs for smoking initiation and ASD, the transmitted PGSs for age at first birth, EA, and
390 wellbeing spectrum, and the non-transmitted by mother PGSs for age at smoking initiation and
391 loneliness. The 13 PGSs (36.1%) included in cluster 2 include 3 transmitted PGSs, 6 PGSs non-
392 transmitted by mother, and 4 by father (**Fig. 2b; Table S9**). This cluster encompasses the transmitted
393 PGSs for age of smoking initiation, loneliness, and smoking initiation, both the non-transmitted PGSs

394 for childhood IQ, intelligence, self-reported health, and wellbeing spectrum, and the non-
395 transmitted by mother PGSs of age at first birth and EA. We observed that the PGSs for wellbeing
396 spectrum, smoking initiation, age at first birth, and age at smoking initiation are not assigned to the
397 same cluster, but included across clusters 1 and 2 (**Fig. 2b; Table S9**). For these four traits, we
398 observed a high number of opposite directions in the correlations among the metabolites and the
399 transmitted and non-transmitted PGSs, i.e., 66.7%, 100%, 76.7%, and 62.2%, respectively (**Fig. 2b;**
400 **Data S6; Table S10**).

401 The metabolite cluster 1 contains 46 metabolites (51.1%), all amines (76.7% of all amines) (**Fig.**
402 **2b; Table S9**). The remaining 14 amines, as well as all steroids and organic acids, are included in
403 metabolite cluster 2 ($N = 44$, 48.9%, **Fig. 2b; Table S9**). Despite these differences, these clusters are
404 still similar to those observed in the DNA methylation-metabolomics model, with 46 (66.7%) and 21
405 (47.7%) overlapping metabolites included in cluster 1 and 2, respectively.

406 Overall, we observed correlations ranging from -0.18 to 0.26 for the PGSs in cluster 1 with
407 metabolites ($r_M = 0.015$, $r_{SD} = 0.02$), and from -0.24 to 0.19 for the cluster 2 PGSs with metabolites
408 ($r_M = -0.03$, $r_{SD} = 0.02$; **Fig. 2b; Data S6; Table S9**). We observed the highest positive correlations (r
409 ≥ 0.20) between the non-transmitted by father ADHD (ADHD_NTf) and smoking initiation PGSs
410 (smokinginitiation_NTf) with both essential and non-essential amino acids, such as L-leucine or L-
411 alanine (ADHD_NTf $r_M = 0.21$, $r_{SD} = 0.01$, r range: 0.21-0.22, smokinginitiation_NTf $r_M = 0.22$, r_{SD}
412 $= 0.02$, r range: 0.20-0.26). Similarly, the most negative correlations ($r \leq -0.20$) were observed
413 between amino acids and the non-transmitted by father PGSs for intelligence (intelligence_NTf) and
414 self-reported health (selfreportedhealth_NTf, intelligence_NTf $r_M = -0.21$, $r_{SD} = 0.01$, r range: -0.22
415 to -0.21, selfreportedhealth_NTf $r_M = -0.21$, $r_{SD} = 0.01$, r range: -0.22 to -0.20). This shows that
416 characteristics tagged by ADHD, smoking initiation, intelligence, and self-reported health correlated
417 to parental construction of environments influencing offspring urinary amino acid levels.

418 Pairwise PGSs-DNA methylation correlations

419 For the pairwise PGSs-DNA methylation model, we again applied hierarchical clustering to find
420 two clusters for the PGSs and DNA methylation data (**Fig. 2c; Data S7**). PGS cluster 1 contains 22 of
421 the PGSs (61.1%) selected by the sPLS-DA model for childhood aggression (**Fig. 2c; Data S7**). This
422 cluster contains 6 transmitted PGSs, 9 PGSs non-transmitted by mother and 7 non-transmitted by
423 father, including the transmitted and both non-transmitted PGSs for ADHD, and MDD, the
424 transmitted and the non-transmitted by mother PGSs for smoking initiation, and wellbeing
425 spectrum, both the non-transmitted PGSs for aggression, and number of cigarettes per day, the
426 transmitted PGSs for age at first birth, and EA, the non-transmitted by mother PGSs for age of
427 smoking initiation, insomnia, and loneliness, and the non-transmitted by father PGSs for ASD,
428 childhood IQ, and intelligence. The 14 PGSs (38.9%) included in cluster 2 include 5 transmitted PGSs,
429 6 PGSs non-transmitted by mother, and 3 by father. This cluster encompasses both the non-
430 transmitted PGSs for self-reported health, the transmitted PGSs for age smoking initiation,
431 aggression, number of cigarettes per day, insomnia, and loneliness, the non-transmitted by mother
432 PGSs for age at first birth, ASD, childhood IQ, EA, and intelligence, and the non-transmitted by father
433 PGSs for smoking initiation, and wellbeing spectrum. The clusters as identified in this model are
434 highly similar to those observed in the PGSs-metabolomics model, with 16 (69.6%) and 9 (69.2%)
435 overlapping PGSs included in cluster 1 and 2, respectively (**Table S9; Data S7**). Although the PGSs-
436 metabolomics and PGSs-DNA methylation models produce very similar clusters for the PGSs, we
437 observe that only the PGSs for self-reported health, ADHD, and MDD were assigned to the same
438 cluster, while the PGSs of only four traits had not been assigned the same cluster in the PGSs-
439 metabolomics model (**Table S9; Data S7**).

440 The DNA methylation cluster 1 contains 1,142 (70.8%) of the CpGs selected by the sPLS-DA
441 models for childhood aggression, and shows the strongest trait enrichments for household
442 socioeconomic status in childhood (OR = 12.58, $p = 3.68 \times 10^{-14}$), and psoriasis (OR = 3.73, $p = 9.55 \times 10^{-11}$;
443 **Table S11**). The 472 (29.2%) CpGs included in cluster 2 show the strongest trait enrichment for

444 glucocorticoid exposure (OR = 50.00, $p \leq 1.00 \times 10^{-308}$; **Table S11**). The clusters as identified in this
445 model are nearly identical to those observed in the DNA methylation-metabolomics model, with
446 1,142 (99.2%) and 463 (98.1%) overlapping CpGs included in cluster 1 and 2, respectively (**Data S4**;
447 **Data S7**).

448 The correlations of PGSs in cluster 1 and 2 with the CpGs ranged from -0.10 to 0.15 ($r_M = 0.02$, r
449 $SD = 0.02$) and from -0.19 to 0.11 ($r_M = -0.03$, $r_{SD} = 0.02$), respectively, and the correlations of the
450 CpGs in cluster 1 and 2 with the PGSs ranged from -0.15 to 0.13 ($r_M = 0.0002$, $r_{SD} = 0.01$) and from
451 -0.19 to 0.15 ($r_M = -0.005$, $r_{SD} = 0.004$), respectively (**Fig. 2c**; **Data S7-S8**). We observed a high
452 number of near zero correlations among the PGSs and CpGs, that likely contribute to the high
453 number of opposite direction correlations among the CpGs and the transmitted and non-transmitted
454 PGSs ($N_M = 906$, $N_{SD} = 499$, $N_{range} = 38-1614$; **Fig. 2c**; **Data S8**; **Table S12**). The most negative
455 correlations ($r \leq -0.15$) were observed between the non-transmitted by father self-reported health
456 PGS with CpGs of cluster 2 ($r_M = -0.18$, $r_{SD} = 0.01$, $r_{range} = -0.19$ to -0.15), and the highest positive
457 correlations ($r \geq 0.15$) between the cluster 2 CpGs and the non-transmitted by father ASD PGS ($r_M =$
458 0.151 , $r_{SD} = 0.001$, $r_{range} = 0.150-0.154$; **Fig. 2c**; **Data S8**). This shows that characteristics tagged by
459 ASD and self-reported health correlated to paternal construction of environments influencing
460 offspring buccal DNA methylation levels.

461 **Multi-omics model for childhood aggression**

462 We built multi-omics panels for childhood aggressive behavior based on multi-block sPLS-DA
463 (MB-sPLS-DA) models, including PGSs, DNA methylation, and metabolomics data. Here, we report
464 the multi-omics model with an empirical design matrix and results for the null and full design
465 matrices can be found in **Appendices C** and **D**, respectively. After cross-validation, the optimal 5-
466 component model included 14 transmitted and 30 non-transmitted PGSs, 746 CpGs, and all 90
467 metabolites, across all components (**Table S5**; **Data S9**). The multi-omics model showed poor
468 separation of aggression cases and controls both across omics blocks and within omics blocks (**Fig.**

469 **S11**). Multi-omics prediction of aggression case-control status in the test data showed an
470 improvement in the prediction (BER = 0.47-0.52; **Table S13**) as compared to single-omics models
471 including only the PGSs or metabolomics data, but not as compared to the model including only the
472 DNA methylation data (**Table S6**). In contrast, in the clinical cohort, the average classification
473 accuracy was poorer in the multi-omics model (BER = 0.53-0.57; **Table S13**) than for the single-omics
474 models (**Table S6**). While the sensitivity and specificity of the multi-omics model was low, ROC curve
475 analyses showed the AUCs ranged from 0.63 to 0.76 in the test data and the clinical cohort (**Table**
476 **S13**), which is an improvement in comparison to the single-omics models (**Table S6**). As for the
477 single-omics models, we observed a low degree of separation among cases and controls in both the
478 test data and in the clinical cohort for the multi-omics model (**Fig. S12-S13**).

479 The multi-omics model selected all 30 non-transmitted PGS, and except for the transmitted PGS
480 for childhood IQ, also all the transmitted PGSs (**Data S9**). Nine of the transmitted and 20 of the non-
481 transmitted PGSs had high average stability, i.e., average of how often the trait was selected across
482 repetitions of the cross-validation folds, to be selected to at least one of the components. The PGSs
483 with high stability included the transmitted and both non-transmitted PGSs for childhood
484 aggression, age at first birth, number of cigarettes per day, intelligence and smoking initiation, the
485 transmitted and non-transmitted by father PGSs for ADHD and insomnia, both the non-transmitted
486 PGSs for age at smoking initiation, EA, and self-reported health, the transmitted PGSs for MDD and
487 wellbeing spectrum, and the non-transmitted by mother PGSs for ASD and childhood IQ.

488 Out of the 746 CpGs selected by the multi-omics model 204 (27.3%) were also selected by the
489 single-omics DNA methylation model, and only cg03469862 (chr11: 68924853) was selected with
490 high stability to any of the components in the multi-omics model (range = 0.10-0.92; **Data S2**; **Data**
491 **S9**). We performed trait enrichment analyses against all reported associations in the EWAS atlas for
492 all selected CpGs in the MB-sPLS-DA model. We observed the strongest enrichment for gender (OR =
493 3.90, $p = 3.97 \times 10^{-31}$), and breast cancer risk (OR = 342.60, $p = 1.44 \times 10^{-21}$; **Table S14**). These CpGs also

494 showed enrichment for e.g., neurological and developmental disorders, such as ASD and Parkinson's
495 disease, cardiometabolic traits, such as obesity and Type II Diabetes, inflammatory disorders, such as
496 respiratory allergies and ankylosis spondylitis, pre- and perinatal risk factors, such as preterm birth
497 and maternal stress, and environmental exposures, such as organophosphate exposure (**Table S14**).
498 All 90 metabolites selected by the MB-sPLS-DA model were selected with high average stability to at
499 least one of the components, and only 11 metabolites showed low stability for selection in any
500 specific component (**Data S9**).

501 Correlations of omics traits selected for childhood aggression in the multi-omics model

502 The average correlations between each omics layer in the multi-omics model, i.e., the
503 correlation among all PLS variates of all components simultaneously, were $r = 0.19$ ($q = 2.13 \times 10^{-27}$)
504 for PGSSs-DNA methylation, $r = 0.13$ ($q = 1.78 \times 10^{-12}$) for PGSSs-metabolomics, and $r = 0.15$ ($q =$
505 3.76×10^{-16}) for DNA methylation-metabolomics. These correlations are lower than those observed
506 for the cross-omics models on which the design matrix was based (**Table S4**), thus, this gives a
507 stronger indication that omics traits from different omics levels capture largely independent
508 information for childhood aggression. We observed high absolute correlations ($|r| \geq 0.60$) between
509 2 selected PGSSs, 14 CpGs, and 13 metabolite, that we summarize in five sets of correlational patterns
510 (**Fig. 3; Data S10; Table S15**).

511 Correlation pattern 1 comprises high negative correlations of citric and fumaric acid with
512 cg12886033 (chr1:65449013, r citrate = -0.61, r fumarate = -0.62), cg14508705 (chr1:172360182, r
513 citrate = -0.61, r fumarate = -0.62), and cg11710553 (chr4:105892960, r citrate = -0.60, r fumarate = -
514 0.61), and high negative correlations of fumaric acid with cg21432062 (chr3:4908643, $r = -0.60$),
515 cg22848658 (chr6:135354586, $r = -0.60$), and cg15841349 (chr12:129348564, $r = -0.60$; **Fig. 3; Data**
516 **S10; Table S15**). Both citric and fumaric acid are intermediates of the tricarboxylic acid (TCA) cycle.
517 TCA cycle metabolites play a role in histone acetylation, and histone and DNA demethylation
518 (Martínez-Reyes and Chandel 2020). The EWAs atlas only included cg21432062 (**Table S15**), where

519 hypermethylation of this CpG associates with inflammatory bowel disease (IBD). This is in line with
520 studies that report decreased levels of citric and fumaric acid, and other TCA cycle-related
521 metabolites, in the serum, urine, and lesion tissue samples of patients with IBD and related disorders
522 (Ooi et al. 2011; Schicho et al. 2012; Dawiskiba et al. 2014). Thus, our negative correlational pattern
523 seems in line with the observed hypermethylation for cg21432062 and decreased levels of citric and
524 fumaric acid. The CpGs cg12886033, cg14508705, cg15841349, and cg22848658 are in the gene
525 bodies of Long Intergenic Non-Protein Coding RNA 1359 (*LINC01359*), Dynamamin 3 (*DNM3*),
526 Glycosyltransferase 1 Domain Containing 1 (*GLT1D1*), and HBS1 Like Translational GTPase (*HBS1L*),
527 respectively. CpGs in these genes associate with traits such as smoking, aging, down syndrome, and
528 various types of cancers (**Table S15**).

529 The second correlational pattern is characterized by high negative correlations between
530 isocitrate with cg05056638 (chr8:24800824, $r = -0.60$), cg08415582 (chr8:57030523, $r = -0.60$),
531 cg11206167 (chr5:42924367, $r = -0.60$), and cg20704654 (chr20:30072118, $r = -0.61$; **Fig. 3; Data**
532 **S10; Table S15**). All four CpGs associate with gender, with additional associations observed for
533 cg05056638 with arsenic exposure (in utero) and Leukoaraiosis, and of cg20704654 with ageing
534 (**Table S15**). The observation that these CpGs correlated highly with isocitrate is in line with research
535 that reported inclusion of plasma isocitrate in the metabolomics profile that predicts chronological
536 age in males and shows higher concentrations in older males (Rist et al. 2017).

537 Correlation pattern 3 contains the high positive correlation of homocysteine with cg13784456
538 (chr10:132970405, $r = 0.84$) and cg06144718 (chr10:133048392, $r = 0.75$; **Fig. 3; Data S10; Table**
539 **S15**). These CpGs are included in the gene body of Transcription Elongation Regulator 1 Like
540 (*TCERG1L*) and the EWAS atlas reported associations of CpGs in this gene with traits such as smoking,
541 infertility, and various types of cancer (**Table S15**). We hypothesize that correlation pattern 3 may
542 reflect the DNA methylation process itself, as homocysteine is involved in the methionine cycle that
543 transfers the methionine methyl group to DNA methyltransferase (Selhub 1999).

544 The fourth correlational pattern includes high positive correlations between cg03469862
545 (chr11:68924853) with the transmitted PGS for ADHD ($r = 0.61$), 3-methoxytyrosine ($r = 0.63$), L-
546 isoleucine ($r = 0.66$), L-leucine ($r = 0.65$), L-phenylalanine ($r = 0.70$), L-tryptophan ($r = 0.60$), L-valine (r
547 $= 0.69$), L-glutamine ($r = 0.70$), L-tyrosine ($r = 0.63$), and L-serine ($r = 0.69$; **Fig. 3; Data S10; Table**
548 **S15**). Look-up in the EWAS atlas showed that cg03469862 associates with prostate cancer and pre-
549 and post-lenalidomide treatment in patients with Myelodysplastic syndrome with isolated deletion
550 (5q) (**Table S15**). That higher DNA methylation of a CpG associated with prostate cancer and
551 Myelodysplastic syndrome is associated with higher metabolite levels, and specifically higher amino
552 acid levels, is corroborated by urinary metabolomics studies that report altered levels of 15
553 metabolites in patients with prostate cancer, including increased levels of valine (Lima et al. 2021),
554 and of 29 metabolites in Myelodysplastic syndrome patients, including increased levels of valine
555 (Yuan et al. 2021). In contrast, prostate cancer patients had decreased urinary levels of serine,
556 leucine, glutamine, and tyrosine (Lima et al. 2021).

557 The final correlation pattern comprises a high negative correlation between the non-
558 transmitted by father PGS for EA and cg09674340 (chr1:202509286, $r = -0.65$; **Fig. 3; Data S10; Table**
559 **S15**). This CpG is located in the 1st exon of the Protein Phosphatase 1 Regulatory Subunit 12B
560 (*PPP1R12B*) gene. CpGs in this gene associate with traits such as gender, smoking, and low birth
561 weight (**Table S15**). The negative association of a smoking-related CpG with indirect genetic effects
562 for EA is in line with a previous study that reported significant negative genetic correlations of
563 indirect parental EA effect with smoking initiation, number of cigarettes per day, and smoking
564 cessation (Wu et al. 2021). Similarly, the phenotypic association of low paternal educational
565 attainment with low offspring birth weight is well-established (e.g., Meng and Groth 2018).

566 Discussion

567 This study comprised an integrative multi-omics analysis of childhood aggressive behavior to
568 identify a multi-omics biomarker panel and to investigate the correlations among the omics traits

569 included in this panel. In our training data comprising 645 twins (cases = 42.0%, controls = 58.0%) we
570 applied multivariate statistical methods to analyze and integrate transmitted and paternal and
571 maternal non-transmitted PGSs for childhood aggression and for 14 traits genetically correlated with
572 aggression (45 PGSs total), 78,772 CpGs, and 90 metabolites (Fig. 1). We build single-omics
573 biomarker panels for each of the omics layers, that selected 31 PGSs, 1,614 CpGs, and 90
574 metabolites to discriminate between aggression cases and controls. The markers selected in single-
575 omics models had poor predictive performance in our test ($N = 277$, cases = 42.2%, controls = 57.8%)
576 and validation data ($N = 142$, cases = 45.1%, controls = 54.9%). The multi-omics panel selected 44
577 PGSs, 746 CpGs, and 90 metabolites, which also had poor predictive performance in our test and
578 validation data.

579 We explored the pairwise correlations of the omics traits selected by the single-omics models.
580 The average correlations between omics layers ranged from $r = 0.18$ to $r = 0.28$. Clustering analyses
581 of each omics layer included in the pairwise correlations showed high overlap in the traits included
582 in each cluster for the same omics layers. We frequently observed that transmitted and non-
583 transmitted PGSs for the same traits were assigned to different clusters, though does not seem
584 related to opposite correlations when comparing transmitted and non-transmitted PGSs, as all PGS
585 traits show such patterns ($N M = 49$, $N SD = 23$, N range: 10-90). We showed that indirect genetic
586 effects for ADHD, ASD, intelligence, smoking initiation, and self-reported health, correlate most
587 strongly with buccal DNA methylation and urinary amino acid levels in children and that higher
588 amino acid levels associate with hypomethylation in a cluster of CpG sites. We described five sets of
589 correlational patterns with high absolute correlations ($|r| \geq 0.60$) of aggression-related omics traits
590 selected by the multi-omics model. These multi-omics correlational patterns associate with a range
591 of traits that link aggression-related omics traits to biological processes related to inflammation,
592 carcinogens, ageing, sex differentiation, intelligence, and smoking.

593 This is the first multi-omics study that includes DNA methylation profiles from buccal and
594 metabolomics in urine. Most of the earlier large-scale omics studies were conducted in blood
595 samples. By obtaining omics measurements in easily accessible peripheral tissues (urine and buccal-
596 cells) we could obtain multi-omics data for more individuals than most previous multi-omics studies
597 for psychiatric traits, such as depression and suicide risk (Bhak et al. 2019) or post-traumatic stress
598 disorder (Dean et al. 2019), that relied on small training samples (range: 126-165). In evaluating the
599 validity of the PGS and multi-omics models in the clinical cohort, the non-transmitted PGSs could not
600 be assessed, as no parental genotypes were available in the clinical cohort. Additional validation in
601 cohorts with complete omics data that applied the same metabolomics and DNA methylation
602 platforms are of large interest, but currently do not exist. Our design is optimal in nearly all other
603 aspects, as the population and clinical cohorts collected all data, including biomarkers, at the same
604 time, using the same arrays and platforms and with similar protocols.

605 The single- and multi-omics models also selected nearly all the PGSs, with only the transmitted
606 PGSs for ASD, intelligence, childhood IQ, and self-reported health, and the non-transmitted by father
607 PGSs for age at first birth, EA, insomnia, and loneliness not selected to the single-omics model, and
608 the transmitted PGS for childhood IQ not selected to the multi-omics model (empirical design
609 matrix). The high selection of transmitted PGSs to the biomarker panels likely reflect the genetic
610 correlations of these traits with childhood aggression on which basis we included them in the
611 current study (Ip et al. 2021). By including both transmitted and non-transmitted PGSs in the
612 genomics block, this block captures the effect of parental genotypes on their offspring's rearing
613 environment. The non-transmitted PGSs for various traits, including childhood aggression, were
614 consistently retained in the single- and multi-omics models, which is in line with research that shows
615 associations of parenting styles with childhood aggression (Masud et al. 2019). Previous research
616 reported significant genetic correlations of indirect genetic EA effects with other complex traits (Wu
617 et al. 2021), thus the high selection of non-transmitted PGSs in our model may also reflect their
618 genetic correlations with childhood aggression.

619 In general, CpGs selected in the single- and multi-omics models were selected with low stability,
620 i.e., the same CpGs was infrequently selected to the models across cross-validation folds and
621 repeats. This low selection stability compared to the stability of PGs and metabolites, might be
622 explained by the large number of CpGs tested for inclusion in the models as compared to the
623 number of metabolites or PGs. The CpGs in the single- or multi-omics models did not overlap with
624 the top differentially methylated CpGs for physical aggression as observed in buccal-cells (Cecil et al.
625 2018b), and were not significantly associated with aggression in a recent blood-based EWAS meta-
626 analysis (van Dongen et al. 2021). Trait enrichment of the CpGs selected by the single- and multi-
627 omics models reported enrichment of known aggression risk factors, such as socioeconomic status
628 (Miller and Tolan 2019; Bellair et al. 2019; Hendriks et al. 2020), childhood malnutrition (Liu 2004;
629 Vaughn et al. 2016), and pre- and perinatal risk factors (Van Adrichem et al. 2020). Also of interest is
630 the enrichment of glucocorticoid exposure in CpGs selected by the single-omics model and the high
631 correlation between cortisol and cg05153029 (chr20:19769815, $r = 0.61$), that associates with
632 glucocorticoid exposure in the EWAS atlas (null design matrix MB-sPLS-DA model). Cortisol and other
633 hypothalamus-pituitary-adrenal (HPA)-axis molecules have been implicated in aggressive behavior,
634 suggesting a role of the stress response system in aggressive behavior (Hagenbeek et al. 2016).
635 Epigenetic programming of the HPA-axis is influenced by pre- and perinatal factors, such as maternal
636 behavior as observed in rats (Weaver et al. 2004), and maternal stress and early life adversity
637 (Mulligan et al. 2012; Hompes et al. 2013; Jiang et al. 2019), and lower average global DNA
638 methylation levels were reported in patients with Cushing's Syndrome (CS) in remission, a model for
639 long-standing excessive glucocorticoid (cortisol) exposure (Glad et al. 2017). Thus, epigenetic
640 mechanisms may mediate the association between cortisol and childhood aggression, similarly as
641 the DNA methylation mediates the association between cortisol stress reactivity and childhood
642 trauma (Wrigglesworth et al. 2019).

643 The single- and multi-omics models selected all 90 LC- and GC-MS metabolites for inclusion,
644 which might be explained by the low expression differences between aggression cases and controls

645 of the urinary amines and organic acids in this sample (Hagenbeek et al. 2020). Another plausible
646 explanation regards the fact that we generated the metabolomics data on three targeted platforms,
647 chosen because they cover relevant metabolites involved in neurotransmitter, inflammation, and
648 steroid hormone pathways that associate with aggression (Hagenbeek et al. 2016). To date, no
649 metabolomics platform can capture the entire metabolome. In addition, within a platform, technical
650 challenges may cause compounds becoming undetectable or not quantifiable. This was the case for
651 the steroid platform being less successful in quantifying (conjugated) sex hormones. Coverage could
652 also be extended to include other metabolite classes, preferably in a hypothesis-free manner by
653 employing non-targeted metabolomics platforms. The five sets of omics traits with high cross-omics
654 correlations in the multi-omics model contained 13 metabolites. These metabolites comprised 8
655 amino acids (L-glutamine, L-isoleucine, L-leucine, L-phenylalanine, L-serine, L-tryptophan, L-tyrosine,
656 and L-valine), 3 metabolites involved in the TCA cycle (citric acid, fumaric acid, and isocitrate), the
657 dopaminergic trace amine 3-methoxytyrosine, and homocysteine, which is involved in cysteine and
658 methionine metabolism. This is in line with previous studies reporting association of metabolites
659 with aggressive behavior (Gulsun et al. 2016; Hagenbeek et al. 2016, 2020; Chen et al. 2020).

660 We explored how sensitive our results are to different specifications of the design matrices and
661 found that these resulted in similar predictive abilities, but selected different numbers of only
662 partially overlapping PGSs and CpGs (**Appendices C and D**). In line with expectations, the predictive
663 ability of the null design matrix was slightly better than for the empirical design matrix, reflecting
664 that such a model focuses on selecting discriminatory variables (Singh et al. 2019; Duruflé et al.
665 2020). We expected that the model with the full design model sacrificed predictive accuracy to
666 select discriminatory variables that are also highly correlated, but this model had the lowest
667 classification error rate as compared to the models with an empirical or null design matrix in the test
668 and clinical data. Multi-omics models with differently specified design matrices differed not only in
669 how many and which PGSs and CpGs were selected, but each multi-omics model provided unique
670 insight into the correlations among the omics traits selected for their association with childhood

671 aggression. In the current study, we relied on the cross-validation results to select the number of
672 traits and components in the model. However, to aid in biological interpretation, other choices can
673 be made.

674 The low predictive accuracy of our single- and multi-omics models does not preclude the
675 potential utility of these panels for, e.g. drug target identification; while common SNPs near drug
676 targets often explain only small amounts of the phenotypic variance, pharmacological manipulations
677 can be highly effective (Timpson et al. 2018). Thus, our description of the correlations of the PGs,
678 CpGs, and metabolites advances our understanding how childhood aggression-related omics traits
679 are interrelated and could lead to clues for potential drug targets, despite the low predictive
680 accuracy of childhood aggression.

681 By adding a fourth broad exposome block, capturing known risk factors for childhood
682 aggression, such as neighborhood variables (Miller and Tolan 2019), to the multi-omics model, the
683 influence of environmental influences can be explored. Inclusion of other omics layers, such as the
684 transcriptome, proteome, or a microbiome, may give other insights into the biological mechanisms
685 of complex traits like childhood aggression. It should be noted that with the current method,
686 inclusion of additional omics layers will cause an increase in the computational burden. Therefore, a
687 different method to integrate multi-omics data or reduction of the computational burden might be
688 considered. Future studies could consider reducing the number of parameters by including a smaller
689 number of CpGs, by for example including only the top 1% or 5% most variable probes, or by
690 selecting CpGs based on their known association with aggressive behavior, such as the top CpGs
691 from the EWAS meta-analysis for aggressive behavior (van Dongen et al. 2021).

692 Conclusions

693 Our work entails one of the first applications of multi-omics approaches to childhood
694 psychopathology. The approach we used was developed for dichotomous traits and classification

695 purposes but also gives insight into the how different omics levels associate with each other.
696 Classification was poor, whereas the multi-omics associations confirm well known associations
697 between childhood aggression and known risk factors as well as provide novel insight into the
698 correlational structure among omics traits from different omics levels.

699 [Declarations](#)

700 [Acknowledgments](#)

701 The Netherlands Twin Register (NTR) warmly thanks all twin families for their participation. LUMC-
702 Curium thanks all patients and their parents for participating, and clinicians for their support. NTR and
703 LUMC-Curium are grateful to all researchers involved in the data collection for the ACTION Biomarker
704 Study.

705 [Funding](#)

706 The current work is supported by the “Aggression in Children: Unraveling gene-environment
707 interplay to inform Treatment and InterventiON strategies” project (ACTION) and the Consortium on
708 Individual Development (CID). ACTION received funding from the European Union Seventh Framework
709 Program (FP7/2007-2013) under grant agreement no 602768. CID is funded through the Gravitation
710 Program of the Dutch Ministry of Education, Culture, and Science and the Netherlands Organization
711 for Scientific Research (NWO grant number 024-001-003). The Netherlands Twin Register is supported
712 by multiple grants from the Netherlands Organizations for Scientific Research (NWO) and Medical
713 Research (ZonMW): Netherlands Twin Registry Repository (NWO 480-15-001/674); Why some
714 children thrive (OCW Gravity program, NWO-024.001.003); Genetic influences on stability and change
715 in psychopathology from childhood to young adulthood (ZonMw 912-10-020); Twin family database
716 for behavior genomics studies (NWO 480-04-004); Twin research focusing on behavior (NWO 400-05-
717 717); Longitudinal data collection from teachers of Dutch twins and their siblings (NWO 481-08-011),
718 Twin-family-study of individual differences in school achievement (NWO-FES, 056-32-010),

719 Genotype/phenotype database for behavior genetic and genetic epidemiological studies (ZonMw
720 Middelgroot 911-09-032); the Biobank-based integrative omics study (BIOS) funded by BBMRI-NL
721 (NWO projects 184.021.007 and 184.033.111); the European Science Council (ERC) Genetics of Mental
722 Illness (ERC Advanced, 230374, PI Boomsma); Developmental trajectories of psychopathology (NIMH
723 1RC2 MH089995); the Avera Institute for Human Genetics, Sioux Falls, USA; the Royal Netherlands
724 Academy of Science Professor Award (PAH/6635) to D.I.B.. A research visit to the University of
725 Toulouse (France) by F.A.H. was supported by the Faculty of Behavioural and Movement Sciences
726 (FGB) Talent Fund (2019). J.D. is supported by the NWO-funded X-omics project (184.034.019). M.B. is
727 supported by an ERC consolidator grant (WELL-BEING 771057, PI Bartels).

728 [Conflict of Interest](#)

729 C.K. was employed by Good Biomarker Sciences (Leiden, the Netherlands). E.A.E. was employed
730 by the Avera Institute for Human Genetics (Sioux Falls, SD, United States). The remaining authors
731 declare that the research was conducted in the absence of any commercial or financial relationships
732 that could be construed as a potential conflict of interest.

733 [Ethical approval](#)

734 The study was conducted according to the guidelines of the Declaration of Helsinki, and approved
735 by the Central Ethics Committee on Research Involving Human Subjects of the VU University Medical
736 Center, Amsterdam (NTR 25th of May 2007 and ACTION 2013/41 and 2014.252), an Institutional
737 Review Board certified by the U.S. Office of Human Research Protections (IRB number IRB00002991
738 under Federal-wide Assurance- FWA00017598; IRB/institute codes), and the Medical Ethical
739 Committee of Leiden University Medical Center (B17.031, B17.032 and B17.040).

740 [Informed consent](#)

741 Parents provided written informed consent for their children and twin parents provided written
742 informed consent for their own participation.

743 **Consent for publication**

744 Not applicable.

745 **Availability of data**

746 The standardized protocol for large scale collection of urine and buccal-cell samples in the home
747 situation as developed for the ACTION Biomarker Study in children available at [http://www.action-](http://www.action-euproject.eu/content/data-protocols)
748 [euproject.eu/content/data-protocols](http://www.action-euproject.eu/content/data-protocols). The data of the Netherlands Twin Register (NTR) ACTION
749 Biomarker Study may be accessed, upon approval of the data access committee, through the NTR
750 (https://tweelingenregister.vu.nl/information_for_researchers/working-with-ntr-data).

751 **Code availability**

752 Analysis code is available upon request from the corresponding author.

753 **Authors' contributions**

754 Conceptualization, F.A.H., J.D., M.B., S.D. and D.I.B.; methodology, S.D.; formal analysis, F.A.H.,
755 R.P. and J.J.H.; investigation, F.A.H., P.J.R., O.F.C., R.R.J.M.V., M.B. and D.I.B.; resources, A.C.H., C.K.,
756 E.A.E. and T.H.; data curation, C.E.M.B.; writing—original draft preparation, F.A.H., J.D., R.P., M.B.
757 and D.I.B.; writing—review and editing, all authors; visualization, F.A.H.; supervision, J.D., M.B. and
758 D.I.B.; funding acquisition, A.C.H., C.K., O.F.C., V.F., T.H., R.R.J.M.V., M.B. and D.I.B. All authors have
759 read and agreed to the published version of the manuscript.

760 References

- 761 Achenbach TM, Ivanova MY, Rescorla LA (2017) Empirically based assessment and taxonomy of
762 psychopathology for ages 1½–90+ years: Developmental, multi-informant, and multicultural
763 findings. *Compr Psychiatry* 79:4–18. <https://doi.org/10.1016/j.comppsy.2017.03.006>
- 764 Anderson CA, Bushman BJ (2002) Human Aggression. *Annu Rev Psychol* 53:27–51.
765 <https://doi.org/10.1146/annurev.psych.53.100901.135231>
- 766 Barban N, Jansen R, de Vlaming R, et al (2016) Genome-wide analysis identifies 12 loci influencing
767 human reproductive behavior. *Nat Genet* 48:1462–1472. <https://doi.org/10.1038/ng.3698>
- 768 Bartels M, Hendriks A, Mauri M, et al (2018) Childhood aggression and the co-occurrence of
769 behavioural and emotional problems: results across ages 3–16 years from multiple raters in six
770 cohorts in the EU-ACTION project. *Eur Child Adolesc Psychiatry* 27:1105–1121.
771 <https://doi.org/10.1007/s00787-018-1169-1>
- 772 Baselmans BML, Jansen R, Ip HF, et al (2019) Multivariate genome-wide analyses of the well-being
773 spectrum. *Nat Genet* 51:445–451. <https://doi.org/10.1038/s41588-018-0320-8>
- 774 Beck JJ, Hottenga J-J, Mbarek H, et al (2019) Genetic Similarity Assessment of Twin-Family
775 Populations by Custom-Designed Genotyping Array. *Twin Res Hum Genet* 22:210–219.
776 <https://doi.org/10.1017/thg.2019.41>
- 777 Bellair PE, McNulty TL, Piquero AR (2019) Persistent material hardship and childhood physical
778 aggression. *Aggress Violent Behav* 49:101309. <https://doi.org/10.1016/j.avb.2019.07.004>
- 779 Benjamini Y, Hochberg Y (1995) Controlling the false discovery rate: a practical and powerful
780 approach to multiple testing. *J. R. Stat. Soc. B* 57:289–300
- 781 Benyamin B, Pourcain B, Davis OS, et al (2014) Childhood intelligence is heritable, highly polygenic
782 and associated with FBNP1L. *Mol Psychiatry* 19:253–258.

- 783 <https://doi.org/10.1038/mp.2012.184>
- 784 Bhak Y, Jeong H, Cho YS, et al (2019) Depression and suicide risk prediction models using blood-
785 derived multi-omics data. *Transl Psychiatry* 9:262. <https://doi.org/10.1038/s41398-019-0595-2>
- 786 Boomsma DI (2015) Aggression in children: unravelling the interplay of genes and environment
787 through (epi) genetics and metabolomics. *J Pediatr Neonatal Individ Med* 4:e040251.
788 <https://doi.org/10.7363/040251>
- 789 Branje S, Geeraerts S, de Zeeuw EL, et al (2020) Intergenerational transmission: Theoretical and
790 methodological issues and an introduction to four Dutch cohorts. *Dev Cogn Neurosci*
791 45:100835. <https://doi.org/10.1016/j.dcn.2020.100835>
- 792 Braun PR, Tanaka-Sahker M, Chan AC, et al (2019) Genome-wide DNA methylation investigation of
793 glucocorticoid exposure within buccal samples. *Psychiatry Clin Neurosci* 73:323–330.
794 <https://doi.org/10.1111/pcn.12835>
- 795 Cecil CAM, Walton E, Jaffee SR, et al (2018a) Neonatal DNA methylation and early-onset conduct
796 problems: A genome-wide, prospective study. *Dev Psychopathol* 30:383–397.
797 <https://doi.org/10.1017/S095457941700092X>
- 798 Cecil CAM, Walton E, Pingault JB, et al (2018b) DRD4 methylation as a potential biomarker for
799 physical aggression: An epigenome-wide, cross-tissue investigation. *Am J Med Genet Part B*
800 *Neuropsychiatr Genet* 177:746–764. <https://doi.org/10.1002/ajmg.b.32689>
- 801 Chen X, Xu J, Tang J, et al (2020) Dysregulation of amino acids and lipids metabolism in schizophrenia
802 with violence. *BMC Psychiatry* 20:1–11. <https://doi.org/10.1186/s12888-020-02499-y>
- 803 Dawiskiba T, Deja S, Mulak A, et al (2014) Serum and urine metabolomic fingerprinting in diagnostics
804 of inflammatory bowel diseases. *World J Gastroenterol* 20:163–174.
805 <https://doi.org/10.3748/wjg.v20.i1.163>

- 806 Dean KR, Hammamieh R, Mellon SH, et al (2019) Multi-omic biomarker identification and validation
807 for diagnosing warzone-related post-traumatic stress disorder. *Mol Psychiatry*.
808 <https://doi.org/10.1038/s41380-019-0496-z>
- 809 Demontis D, Walters RK, Martin J, et al (2019) Discovery of the first genome-wide significant risk loci
810 for attention deficit/hyperactivity disorder. *Nat Genet* 51:63–75.
811 <https://doi.org/10.1038/s41588-018-0269-7>
- 812 Duruflé H, Selmani M, Ranocha P, et al (2020) A powerful framework for an integrative study with
813 heterogeneous omics data: from univariate statistics to multi-block analysis. *Brief Bioinform*
814 00:1–13. <https://doi.org/10.1093/bib/bbaa166>
- 815 Ehli EA, Abdellaoui A, Fedko IO, et al (2017) A method to customize population-specific arrays for
816 genome-wide association testing. *Eur J Hum Genet* 25:267–270.
817 <https://doi.org/10.1038/ejhg.2016.152>
- 818 Fergusson DM, Horwood LJ, Ridder EM (2005) Show me the child at seven: The consequences of
819 conduct problems in childhood for psychosocial functioning in adulthood. *J Child Psychol*
820 *Psychiatry Allied Discip* 46:837–849. <https://doi.org/10.1111/j.1469-7610.2004.00387.x>
- 821 Galili T (2015) dendextend: An R package for visualizing, adjusting and comparing trees of
822 hierarchical clustering. *Bioinformatics* 31:3718–3720.
823 <https://doi.org/10.1093/bioinformatics/btv428>
- 824 Glad CAM, Andersson-Assarsson JC, Berglund P, et al (2017) Reduced DNA methylation and
825 psychopathology following endogenous hypercortisolism - A genome-wide study. *Sci Rep* 7:1–
826 11. <https://doi.org/10.1038/srep44445>
- 827 Grove J, Ripke S, Als TD, et al (2019) Identification of common genetic risk variants for autism
828 spectrum disorder. *Nat Genet* 51:431–444. <https://doi.org/10.1038/s41588-019-0344-8>
- 829 Guillemin C, Provençal N, Suderman M, et al (2014) DNA Methylation Signature of Childhood Chronic

- 830 Physical Aggression in T Cells of Both Men and Women. *PLoS One* 9:e86822.
- 831 <https://doi.org/10.1371/journal.pone.0086822>
- 832 Gulsun M, Oznur T, Aydemir E, et al (2016) Possible relationship between amino acids, aggression
833 and psychopathy. *Int J Psychiatry Clin Pract* 1501:1–10.
- 834 <https://doi.org/10.3109/13651501.2016.1144771>
- 835 Hagenbeek FA, Kluff C, Hankemeier T, et al (2016) Discovery of biochemical biomarkers for
836 aggression: A role for metabolomics in psychiatry. *Am J Med Genet Part B Neuropsychiatr*
837 *Genet* 171:719–732. <https://doi.org/10.1002/ajmg.b.32435>
- 838 Hagenbeek FA, Roetman PJ, Pool R, et al (2020) Urinary Amine and Organic Acid Metabolites
839 Evaluated as Markers for Childhood Aggression: The ACTION Biomarker Study. *Front Psychiatry*
840 11: <https://doi.org/10.3389/fpsyt.2020.00165>
- 841 Hendriks AM, Finkenauer C, Nivard MG, et al (2020) Comparing the genetic architecture of childhood
842 behavioral problems across socioeconomic strata in the Netherlands and the United Kingdom.
843 *Eur Child Adolesc Psychiatry* 29:353–362. <https://doi.org/10.1007/s00787-019-01357-x>
- 844 Hompes T, Izzi B, Gellens E, et al (2013) Investigating the influence of maternal cortisol and
845 emotional state during pregnancy on the DNA methylation status of the glucocorticoid
846 receptor gene (NR3C1) promoter region in cord blood. *J Psychiatr Res* 47:880–891.
847 <https://doi.org/10.1016/j.jpsychires.2013.03.009>
- 848 Ip HF, van der Laan CM, Krapohl EML, et al (2021) Genetic association study of childhood aggression
849 across raters, instruments, and age. *Transl Psychiatry* 11:413. [https://doi.org/10.1038/s41398-](https://doi.org/10.1038/s41398-021-01480-x)
850 [021-01480-x](https://doi.org/10.1038/s41398-021-01480-x)
- 851 Jakovljevic M, Jakovljevic I (2019) A Transdisciplinary Integrative Approach for Precision Psychiatry.
852 In: Kim Y-K (ed) *Frontiers in Psychiatry*. Springer Singapore, Singapore, pp 399–428
- 853 Jansen PR, Watanabe K, Stringer S, et al (2019) Genome-wide analysis of insomnia in 1,331,010

- 854 individuals identifies new risk loci and functional pathways. *Nat Genet* 51:394–403.
855 <https://doi.org/10.1038/s41588-018-0333-3>
- 856 Jiang S, Postovit L, Cattaneo A, et al (2019) Epigenetic Modifications in Stress Response Genes
857 Associated With Childhood Trauma. *Front Psychiatry* 10:1–19.
858 <https://doi.org/10.3389/fpsyt.2019.00808>
- 859 Kassing F, Godwin J, Lochman JE, Coie JD (2019) Using Early Childhood Behavior Problems to Predict
860 Adult Convictions. *J Abnorm Child Psychol* 47:765–778. [https://doi.org/10.1007/s10802-018-](https://doi.org/10.1007/s10802-018-0478-7)
861 [0478-7](https://doi.org/10.1007/s10802-018-0478-7)
- 862 Kong A, Thorleifsson G, Frigge ML, et al (2018) The nature of nurture: Effects of parental genotypes.
863 *Science* (80-) 359:424–428. <https://doi.org/10.1126/science.aan6877>
- 864 Lê Cao KA, Boitard S, Besse P (2011) Sparse PLS discriminant analysis: Biologically relevant feature
865 selection and graphical displays for multiclass problems. *BMC Bioinformatics* 12:.
866 <https://doi.org/10.1186/1471-2105-12-253>
- 867 Lee JJ, Wedow R, Okbay A, et al (2018) Gene discovery and polygenic prediction from a genome-
868 wide association study of educational attainment in 1.1 million individuals. *Nat Genet* 50:1112–
869 1121. <https://doi.org/10.1038/s41588-018-0147-3>
- 870 Li M, Zou D, Li Z, et al (2019) EWAS Atlas: A curated knowledgebase of epigenome-wide association
871 studies. *Nucleic Acids Res*. <https://doi.org/10.1093/nar/gky1027>
- 872 Ligthart L, van Beijsterveldt CEM, Kevenaar ST, et al (2019) The Netherlands Twin Register:
873 Longitudinal Research Based on Twin and Twin-Family Designs. *Twin Res Hum Genet* 1–14.
874 <https://doi.org/10.1017/thg.2019.93>
- 875 Lima AR, Pinto J, Amaro F, et al (2021) Advances and Perspectives in Prostate Cancer Biomarker
876 Discovery in the Last 5 Years through Tissue and Urine Metabolomics. *Metabolites* 11:181.
877 <https://doi.org/10.3390/metabo11030181>

- 878 Liu J (2004) Malnutrition at Age 3 Years and Externalizing Behavior Problems at Ages 8, 11, and 17
879 Years. *Am J Psychiatry* 161:2005–2013. <https://doi.org/10.1176/appi.ajp.161.11.2005>
- 880 Liu M, Jiang Y, Wedow R, et al (2019) Association studies of up to 1.2 million individuals yield new
881 insights into the genetic etiology of tobacco and alcohol use. *Nat. Genet.* 51:237–244
- 882 Martínez-Reyes I, Chandel NS (2020) Mitochondrial TCA cycle metabolites control physiology and
883 disease. *Nat Commun* 11:1–11. <https://doi.org/10.1038/s41467-019-13668-3>
- 884 Masud H, Ahmad MS, Cho KW, Fakhr Z (2019) Parenting Styles and Aggression Among Young
885 Adolescents: A Systematic Review of Literature. *Community Ment Health J* 55:1015–1030.
886 <https://doi.org/10.1007/s10597-019-00400-0>
- 887 Meng Y, Groth SW (2018) Fathers Count: The Impact of Paternal Risk Factors on Birth Outcomes.
888 *Matern Child Health J* 22:401–408. <https://doi.org/10.1007/s10995-017-2407-8>
- 889 Miller GM, Tolan PH (2019) The influence of parenting practices and neighborhood characteristics on
890 the development of childhood aggression. *J Community Psychol* 47:135–146.
891 <https://doi.org/10.1002/jcop.22105>
- 892 Mitjans M, Seidel J, Begemann M, et al (2019) Violent aggression predicted by multiple pre-adult
893 environmental hits. *Mol Psychiatry* 24:1549–1564. <https://doi.org/10.1038/s41380-018-0043-3>
- 894 Moran S, Arribas C, Esteller M (2016) Validation of a DNA methylation microarray for 850,000 CpG
895 sites of the human genome enriched in enhancer sequences. *Epigenomics* 8:389–399.
896 <https://doi.org/10.2217/epi.15.114>
- 897 Mulligan CJ, D’Errico NC, Stees J, Hughes DA (2012) Methylation changes at NR3C1 in newborns
898 associate with maternal prenatal stress exposure and newborn birth weight. *Epigenetics*
899 7:853–857. <https://doi.org/10.4161/epi.21180>
- 900 Odintsova V V., Roetman PJ, Ip HF, et al (2019) Genomics of human aggression. *Psychiatr Genet*

- 901 29:170–190. <https://doi.org/10.1097/YPG.0000000000000239>
- 902 Ooi M, Nishiumi S, Yoshie T, et al (2011) GC/MS-based profiling of amino acids and TCA cycle-related
903 molecules in ulcerative colitis. *Inflamm Res* 60:831–840. [https://doi.org/10.1007/s00011-011-](https://doi.org/10.1007/s00011-011-0340-7)
904 0340-7
- 905 Pinu FR, Beale DJ, Paten AM, et al (2019) Systems biology and multi-omics integration: Viewpoints
906 from the metabolomics research community. *Metabolites* 9:1–31.
907 <https://doi.org/10.3390/metabo9040076>
- 908 R Core Team R: A language and environment for statistical computing. <https://www.r-project.org/>
- 909 Radwan K, Coccaro EF (2020) Comorbidity of disruptive behavior disorders and intermittent
910 explosive disorder. *Child Adolesc Psychiatry Ment Health* 14:24.
911 <https://doi.org/10.1186/s13034-020-00330-w>
- 912 Rist MJ, Roth A, Frommherz L, et al (2017) Metabolite patterns predicting sex and age in participants
913 of the Karlsruhe Metabolomics and Nutrition (KarMeN) study. *PLoS One* 12:1–21.
914 <https://doi.org/10.1371/journal.pone.0183228>
- 915 Rogers P, Stoner J (2016) Modification of the Sandwich Estimator in Generalized Estimating
916 Equations with Correlated Binary Outcomes in Rare Event and Small Sample Settings. *Am J Appl*
917 *Math Stat* 3:243–251. <https://doi.org/110.1016/j.bbi.2017.04.008>
- 918 Rohart F, Gautier B, Singh A, Lê Cao KA (2017) mixOmics: An R package for ‘omics feature selection
919 and multiple data integration. *PLoS Comput Biol* 13:1–20.
920 <https://doi.org/10.1371/journal.pcbi.1005752>
- 921 Savage JE, Jansen PR, Stringer S, et al (2018) Genome-wide association meta-analysis in 269,867
922 individuals identifies new genetic and functional links to intelligence. *Nat Genet* 50:912–919.
923 <https://doi.org/10.1038/s41588-018-0152-6>

- 924 Schicho R, Shaykhtudinov R, Ngo J, et al (2012) Quantitative metabolomic profiling of serum, plasma,
925 and urine by ¹H NMR spectroscopy discriminates between patients with inflammatory bowel
926 disease and healthy individuals. *J Proteome Res* 11:3344–3357.
927 <https://doi.org/10.1021/pr300139q>
- 928 Selhub J (1999) Homocystein Metabolism. *Annu Rev Nutr* 19:217–246.
929 <https://doi.org/10.1146/annurev.nutr.19.1.217>
- 930 Siever LJ (2008) Neurobiology of Aggression and Violence. *Am J Psychiatry* 165:429–442
- 931 Singh A, Shannon CP, Gautier B, et al (2019) DIABLO: An integrative approach for identifying key
932 molecular drivers from multi-omics assays. *Bioinformatics* 35:3055–3062.
933 <https://doi.org/10.1093/bioinformatics/bty1054>
- 934 Sinke L, van Iterson M, Cats D, et al DNAMArray: Streamlined workflow for the quality control,
935 normalization, and analysis of Illumina methylation array data.
936 https://molepi.github.io/DNAMArray_workflow/
- 937 Subramanian I, Verma S, Kumar S, et al (2020) Multi-omics Data Integration, Interpretation, and Its
938 Application. *Bioinform Biol Insights* 14:117793221989905.
939 <https://doi.org/10.1177/1177932219899051>
- 940 Tibshirani R (1996) Regression Shrinkage and Selection via the Lasso. *J R Stat Soc Ser B (Methodol)*
941 58:267–288
- 942 Timpson NJ, Greenwood CMT, Soranzo N, et al (2018) Genetic architecture: the shape of the genetic
943 contribution to human traits and disease. *Nat Rev Genet* 19:110–124.
944 <https://doi.org/10.1038/nrg.2017.101>
- 945 Van Adrichem DS, Huijbregts SCJ, Van Der Heijden KB, et al (2020) Aggressive behavior during
946 toddlerhood: Interrelated effects of prenatal risk factors, negative affect, and cognition. *Child*
947 *Neuropsychol* 26:982–1004. <https://doi.org/10.1080/09297049.2020.1769582>

- 948 van der Laan CM, Morosoli-García JJ, van de Weijer SGA, et al (2021) Continuity of Genetic Risk for
949 Aggressive Behavior Across the Life-Course. *Behav Genet*. [https://doi.org/10.1007/s10519-021-](https://doi.org/10.1007/s10519-021-10076-6)
950 10076-6
- 951 van Dongen J, Hagenbeek FA, Suderman M, et al (2021) DNA methylation signatures of aggression
952 and closely related constructs: A meta-analysis of epigenome-wide studies across the lifespan.
953 *Mol Psychiatry* 2020.07.22.215939. <https://doi.org/10.1038/s41380-020-00987-x>
- 954 Vaughn M, Salas-Wright C, Naeger S, et al (2016) Childhood Reports of Food Neglect and Impulse
955 Control Problems and Violence in Adulthood. *Int J Environ Res Public Health* 13:389.
956 <https://doi.org/10.3390/ijerph13040389>
- 957 Vuoksima E, Rose RJ, Pulkkinen L, et al (2020) Higher aggression is related to poorer academic
958 performance in compulsory education. *J Child Psychol Psychiatry*.
959 <https://doi.org/10.1111/jcpp.13273>
- 960 Watanabe K, Stringer S, Frei O, et al (2019) A global overview of pleiotropy and genetic architecture
961 in complex traits. *Nat Genet* 51:1339–1348. <https://doi.org/10.1038/s41588-019-0481-0>
- 962 Weaver ICG, Cervoni N, Champagne FA, et al (2004) Epigenetic programming by maternal behavior.
963 *Nat Neurosci* 7:847–854. <https://doi.org/10.1038/nn1276>
- 964 Whipp AM, Korhonen T, Raevuori A, et al (2019) Early adolescent aggression predicts antisocial
965 personality disorder in young adults: a population-based study. *Eur Child Adolesc Psychiatry*
966 28:341–350. <https://doi.org/10.1007/s00787-018-1198-9>
- 967 Whipp AM, Vuoksima E, Bolhuis K, et al (2021a) Teacher-rated aggression and co-occurring
968 behaviors and emotional problems among schoolchildren in four population-based European
969 cohorts. *PLoS One* 16:e0238667. <https://doi.org/10.1371/journal.pone.0238667>
- 970 Whipp AM, Vuoksima E, Korhonen T, et al (2021b) Ketone body 3-hydroxybutyrate as a biomarker
971 of aggression. *Sci Rep* 11:5813. <https://doi.org/10.1038/s41598-021-84635-6>

- 972 Wörheide MA, Krumsiek J, Kastenmüller G, Arnold M (2021) Multi-omics integration in biomedical
973 research – A metabolomics-centric review. *Anal Chim Acta* 1141:144–162.
974 <https://doi.org/10.1016/j.aca.2020.10.038>
- 975 Wray NR, Ripke S, Mattheisen M, et al (2018) Genome-wide association analyses identify 44 risk
976 variants and refine the genetic architecture of major depression. *Nat Genet* 50:668–681.
977 <https://doi.org/10.1038/s41588-018-0090-3>
- 978 Wrigglesworth J, Ancelin ML, Ritchie K, Ryan J (2019) Association between DNA methylation of the
979 KITLG gene and cortisol levels under stress: a replication study. *Stress* 22:162–168.
980 <https://doi.org/10.1080/10253890.2018.1519019>
- 981 Wu Y, Zhong X, Lin Y, et al (2021) Estimating genetic nurture with summary statistics of
982 multigenerational genome-wide association studies. *Proc Natl Acad Sci* 118:e2023184118.
983 <https://doi.org/10.1073/pnas.2023184118>
- 984 Yuan Y, Zhao J, Li T, et al (2021) Integrative metabolic profile of myelodysplastic syndrome based on
985 UHPLC–MS. *Biomed Chromatogr* 1–12. <https://doi.org/10.1002/bmc.5136>
- 986

987 **Figures**

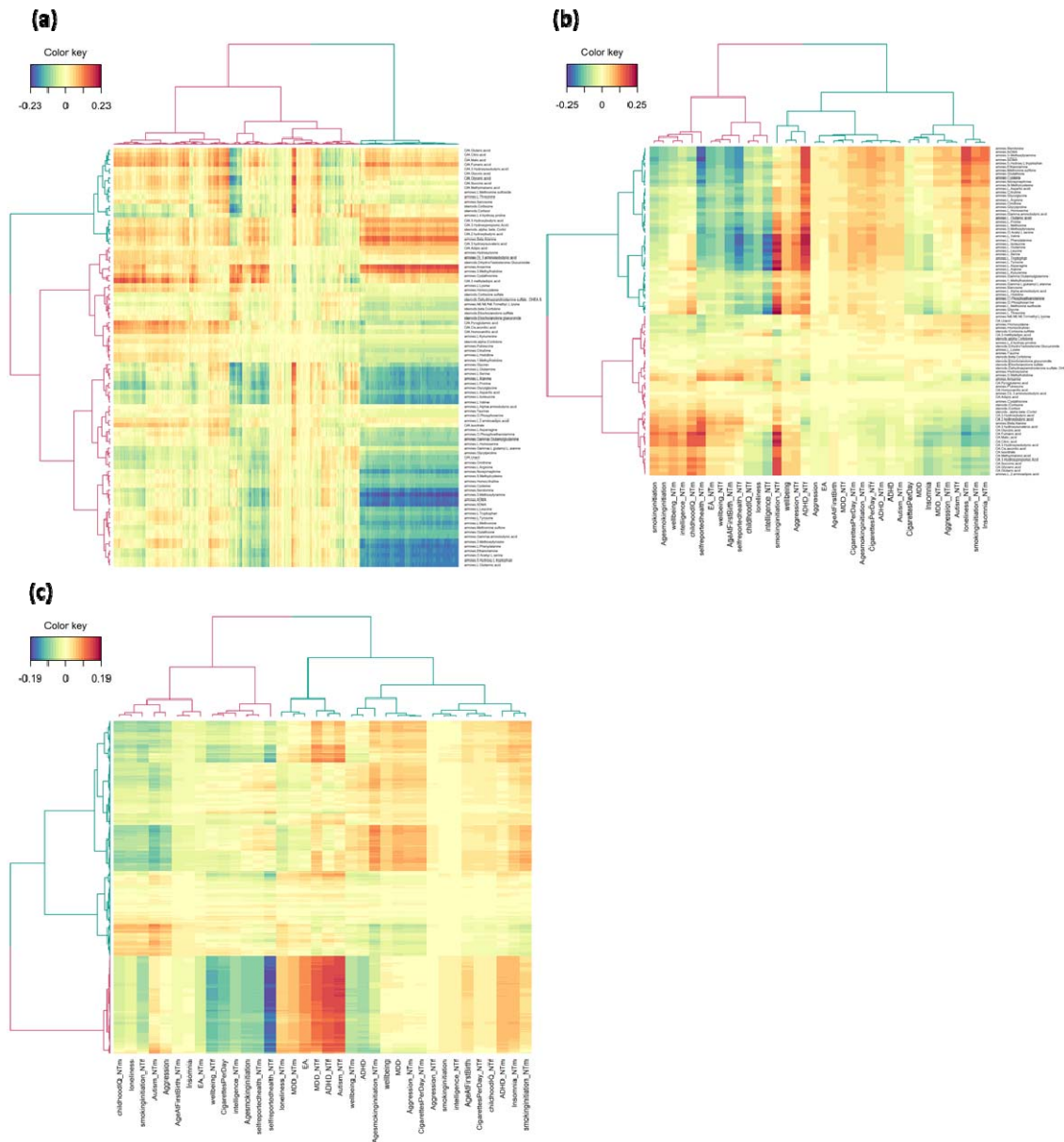
988 **Fig. 1.** Overview of the biomarker identification approach for childhood aggression—details of
989 statistical analyses and data included in each analysis.

990 We employed an analytical design comprising three phases: 1) single-omics analyses; 2) pairwise
991 cross-omics analyses; and 3) multi-omics analyses. First, we performed univariate polygenic score
992 (PGS) analysis in 70% of the twin data and built multivariate single-omics biomarker panels in the
993 twin cohort, with 70% of the twin data for model training (training data), 30% of the twin data for
994 model testing (test data), and the clinical cohort for model validation (validation data). Second, we
995 examined the overall pairwise cross-omics correlations and the pairwise correlations of those omics
996 traits selected by the single-omics models in the training data. Third, using the same data split for
997 model training, testing and validation, we compared three multi-omics models, with different
998 assumptions of the correlations among the omics traits, and describe the multi-omics correlations of
999 the selected omics traits. We offer the analytical details in the **Methods** section.

Study Phase	Analyses	Design
1. Single-omics	<p><u>Univariate:</u></p> <ul style="list-style-type: none"> • Polygenic score analysis <p><u>Multivariate – model training:</u></p> <ul style="list-style-type: none"> • Principal Component Analysis (PCA) • Partial Least Squares Discriminant Analysis (PLS-DA) • Sparse Partial Least Squares Discriminant Analysis (sPLS-DA) <p><u>Multivariate – model testing & validation:</u></p> <ul style="list-style-type: none"> • Predict out-of-sample case-control status • Receiver Operating Characteristic (ROC) analysis 	<p><u>Training data:</u></p> <ul style="list-style-type: none"> • 70% twin cohort ($N = 645$) • <i>Cases</i>: 271 (42.0%) • <i>Controls</i>: 374 (58.0%) <p><u>Test data:</u></p> <ul style="list-style-type: none"> • 30% twin cohort ($N = 277$) • <i>Cases</i>: 117 (42.2%) • <i>Controls</i>: 160 (57.8%) <p><u>Validation data:</u></p> <ul style="list-style-type: none"> • Clinical cohort ($N = 142$) • <i>Cases</i>: 64 (45.1%) • <i>Controls</i>: 78 (54.9%)
2. Pairwise cross-omics	<p><u>All omics traits:</u></p> <ul style="list-style-type: none"> • Partial Least Squares (PLS) analysis <p><u>Selected omics traits:</u></p> <ul style="list-style-type: none"> • Partial Least Squares (PLS) analysis • Hierarchical clustering 	<p><u>Training data:</u></p> <ul style="list-style-type: none"> • 70% twin cohort ($N = 645$) • <i>Cases</i>: 271 (42.0%) • <i>Controls</i>: 374 (58.0%)
3. Multi-omics	<p><u>Model training:</u></p> <ul style="list-style-type: none"> • Multi-block Partial Least Squares Discriminant Analysis (MB-PLS-DA) • Multi-block sparse Partial Least Squares Discriminant Analysis (MB-sPLS-DA) <p><u>Model testing & validation:</u></p> <ul style="list-style-type: none"> • Predict out-of-sample case-control status • Receiver Operating Characteristic (ROC) analysis 	<p><u>Training data:</u></p> <ul style="list-style-type: none"> • 70% twin cohort ($N = 645$) • <i>Cases</i>: 271 (42.0%) • <i>Controls</i>: 374 (58.0%) <p><u>Test data:</u></p> <ul style="list-style-type: none"> • 30% twin cohort ($N = 277$) • <i>Cases</i>: 117 (42.2%) • <i>Controls</i>: 160 (57.8%) <p><u>Validation data:</u></p> <ul style="list-style-type: none"> • Clinical cohort ($N = 142$) • <i>Cases</i>: 64 (45.1%) • <i>Controls</i>: 78 (54.9%)

1001 **Fig. 2.** Clustered heatmaps of the correlations obtained by the pairwise cross-omics Partial Least
1002 Squares (PLS) regression models including only the omics traits as selected by the single-omics
1003 sparse Partial Least Squares Discriminant Analyses (sPLS-DA).

1004 We generated the hierarchical clustering using the Ward linkage algorithm on Euclidean distances of
1005 the PLS variates. For each dendrogram we identified two clusters (cluster 1 = pink, cluster 2 = blue).
1006 We have depicted positive correlations among the omics traits in red and negative correlations in
1007 blue. For the polygenic scores (PGSs), the ‘_NTm’ suffix denotes PGSs non-transmitted by mother,
1008 the ‘_NTf’ suffix denotes the PGSs non-transmitted by father, and childhood aggression is
1009 abbreviated as “aggression”, Attention-Deficit Hyperactivity Disorder as “ADHD”, Major Depressive
1010 Disorder as “MDD”, Autism Spectrum Disorder as “Autism”, Educational Attainment as “EA”, and
1011 wellbeing spectrum as “wellbeing”. For the metabolites, the ‘amines.’ prefix shows we measured
1012 these metabolites on the Liquid Chromatography Mass Spectrometry (LC-MS) amines platform, the
1013 ‘steroids.’ prefix shows we measured these metabolites on the LC-MS steroids platform, and the
1014 ‘OA.’ prefix shows we measured these metabolites on the Gas Chromatography (GC-) MS organic
1015 acids platform. **(a)** Correlation among the 1,614 CpGs and 90 metabolites included in the 3-
1016 component DNA methylation-metabolomics PLS model, where the selected CpGs are represented in
1017 the columns and the metabolomics traits in the rows. We included the cluster assignments and the
1018 full correlation matrix in **Data S4-S5**. **(b)** Correlations among the 36 PGSs and 90 metabolites
1019 included in the 2-component PGSs-metabolomics PLS model, where the selected PGSs are
1020 represented in the columns and the metabolomics traits in the rows. We included the cluster
1021 assignments and the full correlation matrix in **Table S9** and **Data S6**, respectively. **(c)** Correlation
1022 among the 36 PGSs and 1,614 CpGs included in the 2-component PGSs-DNA methylation PLS model,
1023 where the selected PGSs are represented in the columns and the CpGs in the rows. We included the
1024 cluster assignments and the full correlation matrix in **Data S7-S8**.



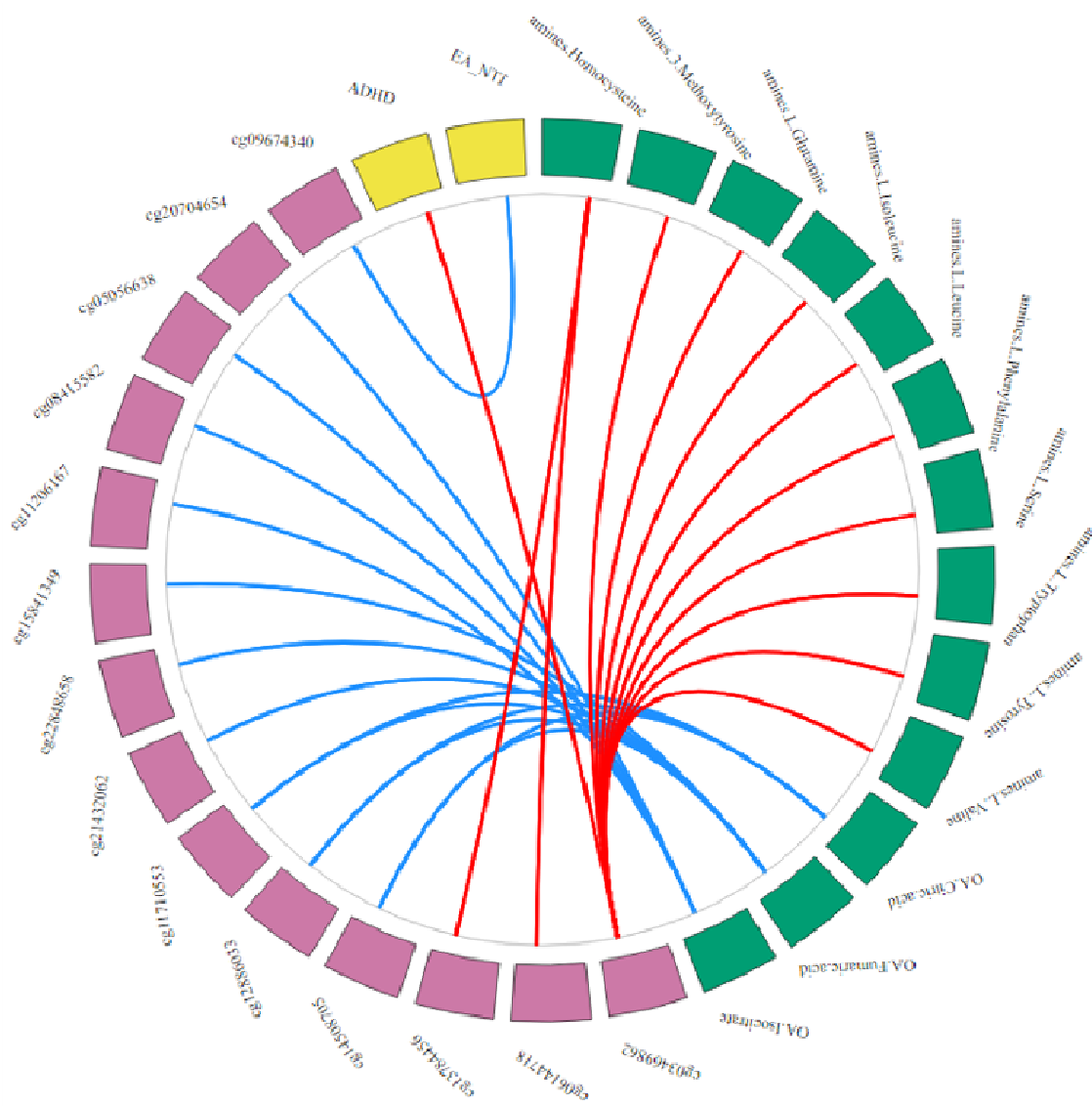
1025

1026 **Fig. 3.** High cross-omics correlations of the multi-omics traits identified in the 5-component multi-
1027 block sparse Partial Least Squares Discriminant Analysis (MB-sPLS-DA) model including the empirical
1028 design matrix

1029 The outer ring depicts the PGSs, CpGs, and metabolites in yellow, pink, and green, respectively. For
1030 the polygenic scores (PGSs), Attention-Deficit Hyperactivity Disorder is abbreviated as “ADHD”, and
1031 Educational Attainment as “EA”, and the ‘_NT’ suffix denotes the PGSs non-transmitted by father.

1032 For the metabolites, the ‘amines.’ prefix shows we measured these metabolites on the Liquid

1033 Chromatography Mass Spectrometry (LC-MS) amines platform, and the 'OA.' prefix shows we
1034 measured these metabolites on the Gas Chromatography (GC-) MS organic acids platform. The inner
1035 plot depicts the correlations among the omics traits. Here, we depict only high absolute correlations
1036 ($|r| \geq 0.60$) between traits of at least two omics layers, with blue lines reflecting negative
1037 correlations and red lines positive correlations. We averaged correlations across all components in
1038 the MB-sPLS-DA model. We included the full correlation matrix in **Data S10** and the correlational
1039 patterns in **Table S15**.



1040
1041

Tables

Table 1. Overview of the discovery genome-wide association studies to calculate polygenetic scores.

Trait ¹	N discovery GWA	Reference	Source original summary statistics
Childhood aggression	151,741	(Ip et al. 2021)	Paper accepted, summary statistics obtained from authors
Attention-Deficit Hyperactivity Disorder	20,183 cases & 35,191 controls	(Demontis et al. 2019)	http://ipsych.au.dk/downloads/data-download-agreement-adhd-european-ancestry-gwas-june-2017
Major Depressive Disorder	135,458 cases & 344,901 controls	(Wray et al. 2018)	https://www.med.unc.edu/pgc/results-and-downloads/
Autism Spectrum Disorder	18,381 cases & 27,969 controls	(Grove et al. 2019)	https://www.med.unc.edu/pgc/results-and-downloads/
Loneliness	355,583	http://www.nealelab.is/uk-biobank/	https://www.dropbox.com/s/nf4jl3mdppu1ng8/2020.gwas.imputed_v3.both_sexes.tsv.bgz?dl=0
Insomnia	1,331,010	(Jansen et al. 2019)	https://ctg.cncr.nl/documents/p1651/Insomnia_sumstats_Jansenetal.txt.gz
Self-reported Health	359,681	http://www.nealelab.is/uk-biobank/	https://www.dropbox.com/s/aawh07hlhldbckc/2178.gwas.imputed_v3.both_sexes.tsv.bgz?dl=0
Smoking initiation (Ever/never smoked)	1,232,091	(Liu et al. 2019)	https://conservancy.umn.edu/bitstream/handle/11299/201564/SmokingInitiation.txt.gz?sequence=27&isAllowed=y
Age of smoking initiation	94,891	(Watanabe et al. 2019)	https://atlas.ctglab.nl/ukb2_sumstats/f.2867.0.0_res.EUR.sumstats.MACfilt.txt.gz
Cigarettes per day	37,334	(Liu et al. 2019)	https://conservancy.umn.edu/bitstream/handle/11299/201564/CigarettesPerDay.txt.gz?sequence=17&isAllowed=y
Childhood IQ	17,989	(Benyamin et al. 2014)	http://sngac.org/documents/CHIC_Summary_Benyamin2014.txt.gz
Educational Attainment ⁵	1,131,881	(Lee et al. 2018)	https://www.dropbox.com/s/ho58e9jmytmpaf8/GWAS_EA_excl23andMe.txt?dl=0
Age at first birth	251,151	(Barban et al. 2016)	http://sociogenome.com/material/GWASresults/AgeFirstBirth_Pooled.txt.gz
Wellbeing spectrum	2,370,390	(Baselmans et al. 2019)	https://surfdive.surf.nl/files/index.php/s/Ow1qCDpFT421ZOO/download?path=%2FMultivariate_GWAMA_sumstats%2FN_GWAMA&files=N_GWAMA_WB_spectrum_no23andME.txt.gz
Intelligence	269,867	(Savage et al. 2018)	https://ctg.cncr.nl/documents/p1651/SavageJansen_IntMeta_sumstats.zip

¹ In the (supplementary) tables and figures childhood aggression is abbreviated as “aggression”, Attention-Deficit Hyperactivity Disorder as “ADHD”, Major Depressive Disorder as “MDD”, Autism Spectrum Disorder as “Autism”, Educational Attainment as “EA”, and wellbeing spectrum as “wellbeing”.

Table 2. Demographics of the training, test, and validation data.

	Training data (70% twin cohort)			Test data (30% twin cohort)			Validation data (Clinical cohort)		
	Controls	Cases	Total	Controls	Cases	Total	Controls	Cases	Total
<i>N</i> (%)	374 (58.0%)	271 (42.0%)	645 (100%)	160 (57.8%)	117 (42.2%)	277 (100%)	78 (54.9%)	64 (45.1%)	142 (100%)
<i>N</i> (%) complete twin pairs	128	80	293	56	35	128	-	-	-
Mean (<i>SD</i>) age	9.4 (1.9)	9.6 (1.8)	9.5 (1.9)	9.6 (1.9)	9.6 (1.9)	9.6 (1.9)	10.8 (1.7)	9.6 (1.7)	10.2 (1.8)
Range age	6.1 - 12.7	6.1 - 12.9	6.1 - 12.9	5.6 - 12.6	5.8 - 12.8	5.6 - 12.8	6.5 - 13.4	6.3 - 13.3	6.3 - 13.4
<i>N</i> (%) females	199 (53.2%)	116 (42.8%)	315 (48.8%)	81 (50.6%)	55 (47.0%)	136 (49.1%)	20 (25.6%)	19 (29.7%)	39 (27.5%)
<i>N</i> (%) MZ twins	299 (80.0%)	228 (84.1%)	527 (81.7%)	118 (73.7%)	108 (92.3%)	226 (81.6%)	-	-	-
Mean (<i>SD</i>) aggression score ¹	3.3 (4.1)	7.3 (5.8)	5.0 (5.3)	3.1 (4.0)	7.6 (6.6)	5.0 (5.7)	6.1 (3.4)	21.1 (4.8)	12.9 (8.5)

Notes: MZ, monozygotic.

¹ Measured with the mother-rated Aggressive Behavior syndrome scale of the Achenbach System of Empirically Based Assessment (ASEBA) Child Behavior Checklist (CBCL). The ASEBA CBCL Aggressive Behavior scores in the clinical cohort include 90% mother report and 10% father report.